www.czasopisma.pan.pl PAN www.journals.pan.pl

Acta Geologica Polonica, Vol. 72 (2022), No. 4, pp. 423–442
DOI: 10.24425/agp.2022.142646

Recently formed arsenates from an abandoned mine in Radzimowice (SW Poland) and the conditions of their formation

RAFAŁ SIUDA and ANNA JANUSZEWSKA

University of Warsaw, Faculty of Geology, Żwirki i Wigury 93, 02-098 Warszawa, Poland;
e-mails: rsiuda@uw.edu.pl, a.januszewska3@uw.edu.pl

ABSTRACT:

Siuda, R. and Januszewska, A. 2022. Recently formed arsenates from an abandoned mine in Radzimowice (SW Poland) and the conditions of their formation. *Acta Geologica Polonica*, **72** (4), 423–442. Warszawa.

In the mining galleries of the abandoned Au-As mine in Radzimowice, diverse groups of secondary arsenates crystallized recently. They form several characteristic assemblages. In the first of them the typical minerals are bukovskýite and melanterite. The second group of secondary arsenates includes scorodite, kaňkite, zýkaite, and pitticite. The third assemblage includes Co-Ni-Mg arsenates of the erythrite-annabergite-hörnesite series. The first assemblage crystallized in a zone with a very high activity of sulphate and arsenate ions and where the pH varies within a narrow range of 2.0–3.5. The second group of secondary arsenates formed in the acidic zone. The minerals identified here suggest pH variation within fairly wide ranges, from about 2.0 to 5.5. Contrary to the first and second mineral assemblage, the Co-Ni-Mg arsenates formed under different geochemical conditions. Their crystallization took place under weak acidic to neutral conditions.

Key words: Bukovskýite; Kaňkite; Zýkaite; Pitticite; Iron arsenates; Oxidation zone; Radzimowice.

INTRODUCTION

Arsenic is an element known for its high toxicity. Its high concentrations appear in both natural geological environments and the areas of intensive anthropopressure (Matschullat 2000; Morin and Calas 2006). Hydrothermal polymetallic deposits stand for a typical environment where high amounts of primary arsenic minerals (e.g., arsenopyrite) occur. Exploitation of polymetallic ores and their processing has lead to the formation of many waste piles with a high concentration of As. Decomposition of primary arsenic minerals takes place within natural zones of weathering, and on post-mining dumps. This process causes the release of significant amounts of arsenic into the environment. This leads to contamination of surrounding ecosystems and negatively affects the quality of local soil and surface waters (Welch *et al.* 2000; Smedley and Kinniburgh 2002; Hering and Kneebone 2002). However, crystallization of secondary iron arsenates may prevent sizable amounts of arsenic from spreading within the environment. Among the secondary arsenic minerals, iron arsenates and iron arsenosulphates play a crucial role in the permanent binding and immobilization of arsenic (Drahota and Filippi 2009; Li *et al.* 2021).

This work presents the results of mineralogical research of secondary iron arsenates and associating phases occurring in the abandoned Au-As-Cu mine in Radzimowice. Based on the conducted research, parageneses of secondary arsenic minerals were described and the conditions under which these minerals crystallize were recreated.

GEOLOGICAL SETTING

The polymetallic Radzimowice deposit is located in the SE part of the Kaczawa Mts. (Text-fig. 1). This area is built of metamorphosed mudrocks of Lower Palaeozoic age belonging to the Kaczawa Metamorphic Complex, which includes the Radzimowice slates and Chmielarz slates. Both lithologies are represented by various quartz-sericite-graphite mudrocks, greywackes, and greenstones containing insets of crystalline limestone and quartzites (Urbanek and Baranowski 1986; Haydukiewicz and Urbanek 1986; Baranowski 1988; Kozdrój *et al.* 2001). The metamorphic rocks are cut by younger intrusions of igneous rocks, mainly rhyolites whose crystallization age has been determined as ca. 315Ma (Machowiak *et al.* 2008; Mikulski and Williams 2014). Within the rhyolites of the Żelaźniak and Bukowinka hills, granites are also found (Machowiak *et al.* 2008; Mikulski 2003). The rarest igneous rocks in this region are andesites and lamprophyres dated to ca. 312 Ma (Mikulski and Williams 2014).

The primary ore occurs mainly in the form of several quartz-sulfide veins, of which six were under exploitation (Manecki 1965; Zimnoch 1965; Paulo and Salomon 1974; Mikulski 2005, 2007). These crack-type veins cut both the metamorphic rocks of the Kaczawa Metamorphic Complex and the later igneous rocks. They run more or less parallel along an E-W direction. The dips of the veins are steep (ca. 60–90º) and mainly directed to the north. The thickness of the veins varies from a few centimetres to more than 1 m. The longest vein – "Pocieszenie Górnika" – is ca. 2 km long and ≤1.4 m thick. The barren rocks surrounding the veins are hydrothermally altered and usually contain disseminated ore minerals.

The primary ore vein mineralogy is diverse. The most common primary ore minerals are: pyrite, arsenopyrite, chalcopyrite, sphalerite, galena, marcasite, tetrahedrite, boulangerite, bournonite, meneghinite, gold, bismuth and tellurium minerals associated with barren minerals such as quartz, rhodochrosite and kutnohorite (e.g., Stauffacher 1916; Manecki 1965; Zimnoch 1965; Sylwestrzak and Wołkowicz 1985; Mikulski 2005, 2007, 2011; Mikulski and Muszyński 2012). The age of the ore mineralization determined by the Re-Os method is 317±17 Ma (Mikulski 2007).

So far 43 minerals have been described from the weathering zone of the Radzimowice deposit. The first information about secondary minerals in Radzimowice was given by Fiedler (1863), who mentioned the occurrence of hematite, pitticite, and chalcocite. Traube

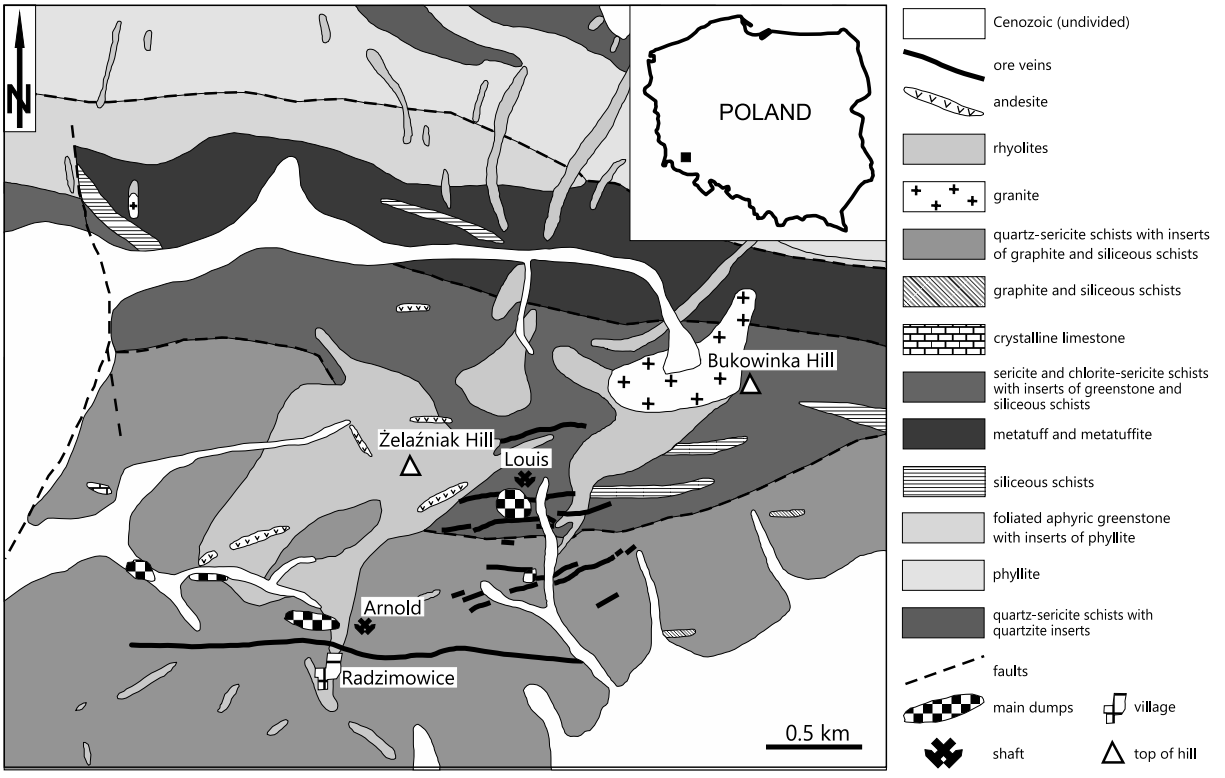

Text-fig. 1. Geological sketch-map of the Radzimowice area (after Cwojdziński and Kozdrój 1994).

(1888) described the occurrence of native copper and limonite. Malachite, and dripstones of "limonite" forming in old mine galleries were reported by Stauffacher (1916). Zimnoch (1965) described cerussite and covellite while cuprite was identified by Manecki (1962). A short note about the presence of pseudomalachite was published by Holeczek and Janeczek (1991). The presence various iron arsenates in Radzimowice was reported by Siuda (2004) and Parafiniuk *et al.* (2016) while mottramite was first mentioned by Siuda and Kruszewski (2005). Parafiniuk and Siuda (2006) also described the occurrence of schwertmannite. A detailed report on selected secondary copper minerals was presented by Siuda and Kruszewski (2013).

The earliest records of mining in Radzimowice come from the 12th century (Dziekoński 1972). Intensive mining exploitation took place in the 19th century and the first half of the 20th century. Finally, the exploitation was finished in 1956. During exploitation, dozens of kilometres of underground mine workings were constructed. The depth of the mine was about 170 metres. The extensive system of mining excavations caused changes in the geochemical conditions prevailing in the rock mass. After the end of mining activities, the abandoned underground mining excavations became the place of the formation of secondary minerals.

METHODS

Samples of weathering minerals were collected from two underground exploitation levels (level II, IIIB) from depths of 50 and 100 metres below ground level. To avoid humidity changes, the mineral samples were packed into tightly-sealed plastic containers. The samples transported to the laboratory were stored at a temperature around +5°C. After this, the samples were dried at room temperature and then ground in an agate mortar. The determination of the mineralogical nature of the samples began with the Powder X-Ray Diffraction (PXRD) technique. The powdered sample was placed in a Bruker D8 ADVANCE equipped with superfast linear position-sensitive detector (LPSD) VÅNTEC-1 and kβ-filtered CoKα radiation. The apparatus is located in the Institute of Geological Sciences, Polish Academy of Sciences. The samples were scanned using 0.02 2θ increment and 1 s/step counting time (equivalent of 416 s in the zero-dimensional detector language), in the 3–80 2θ range. Unit cell parameters were calculated using the Rietveld method implemented in the TOPAS v. 3.0 software. Quantitative chemical data were collected using a Cameca SX 100 electron microprobe of the Inter-Institute Analytical Complex from Minerals and Synthetic Substances, University of Warsaw. The following standards, analytical lines, and crystals were used:, rhodochrosite – Mn (Kα, LIF, detection limit (DL) – 0.15 wt%), Fe_2O_3 – Fe (Kα, LIF, DL – 0.15 wt%), chalcopyrite – Cu (Kα, LIF, DL – 0.23 wt%), ZnS – Zn (Kα, LIF, DL – 0.29 wt%), albite – Na (Kα, TAP, DL – 0.03 wt%, diopside – Mg (Kα, TAP, DL – 0.01 wt%), orthoclase – Al (Kα, TAP, DL – 0.04 wt%), diopside – Si (Kα, TAP, DL – 0.03 wt%), GaAs – As (Lα, TAP, DL – 0.10 wt%), apatite – P (Kα, PET, DL – 0.07 wt%), orthoclase – K (Kα, PET, DL – 0.04 wt%), diopside – Ca (Kα, PET, DL – 0.05 wt%), NiO – Ni (Kα, LIF, DL – 0.04), metallic Co – Co (Kα, LIF, DL – 0.03). Analyses were conducted using the accelerating voltage of 15 kV and beam current of 10 nA. The beam diameter was 5–10 μm. The ZAF corrections were applied. Elevated analytical totals for minerals with hydroxyl groups or crystallization water are generally caused by evaporation of water under high vacuum conditions or by its evaporation due to heating of the analyzed area by the electron beam. Lower totals are due to the porous nature of some minerals. IR absorption spectra were recorded at a Nicolet Magna 550 spectrometer from 4000 to 400 cm^{-1}, using KBr pellets (Faculty of Chemistry, University of Warsaw). Thermal analysis was carried out at a Paulik-Paulik-Erdey derivatograph at a heating rate of 10 °C/min in the air with 200 mg of sample and Al_2O_3 as inert reference material. Measurements of the pH were performed *in situ* by electrochemical methods using appropriate electrodes (Elmetron, Poland).

SECONDARY ARSENIC MINERALS

The following minerals are given according to the frequency of their occurrence. The description starts with arsenic minerals after that the other secondary phases are presented.

Scorodite $FeAsO_4 \cdot 2H_2O$

At the third exploitation level of the mine, scorodite crystallizes in form of botryoidal, grey-green or brown aggregates, up to dozen centimetres in diameter. The mineral covers the walls of mine galleries and creates dripstones (Text-fig. 2A). At high magnifications, elongated bacteria colonies mineralized by scorodite are visible inside minothems (Text-fig. 3A). In the abandoned mine galleries

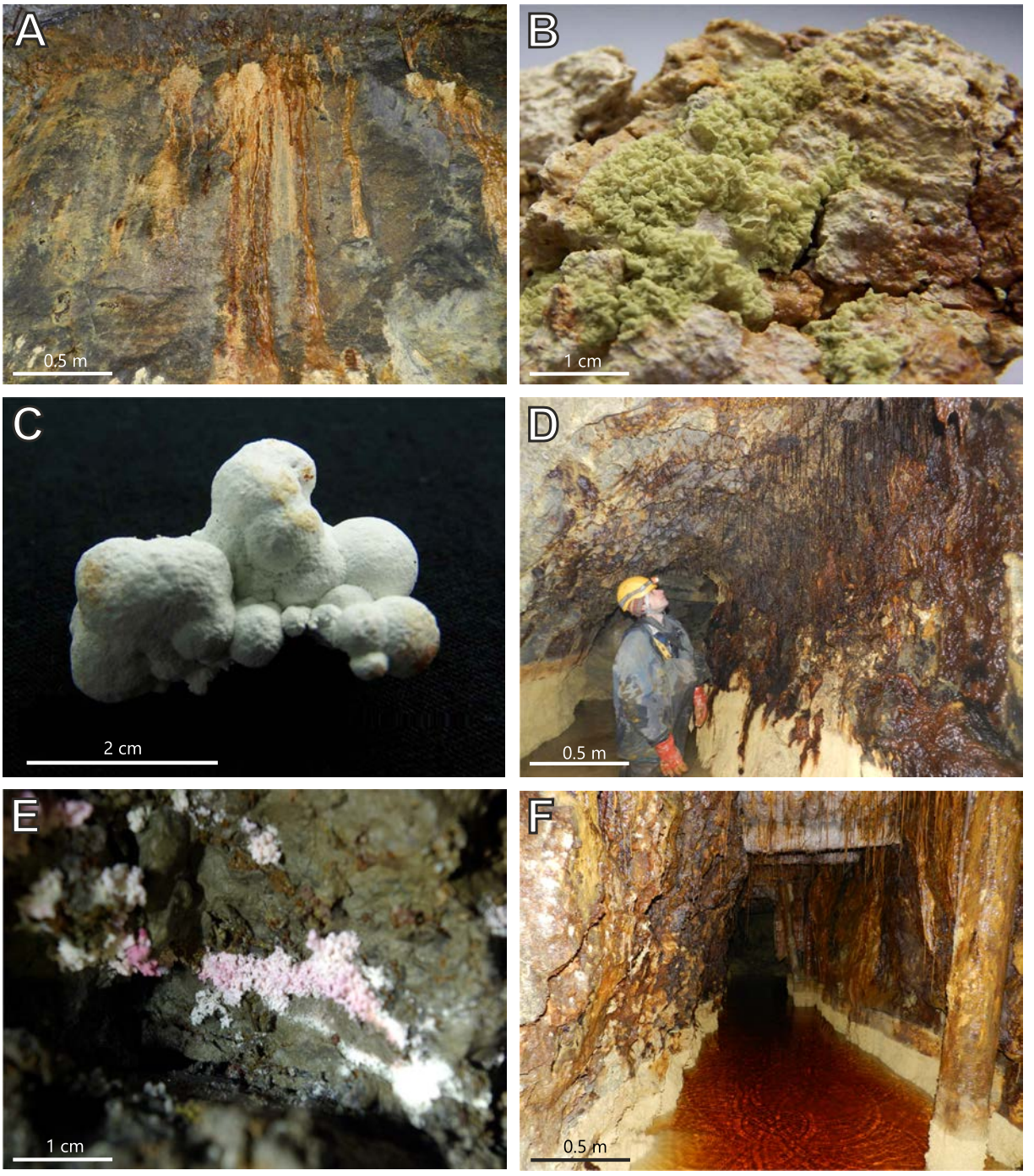

Text-fig. 2. Formation of various secondary arsenic minerals from the abandoned mine in Radzimowice: A – dripstones of scorodite on the mine walls; B – cryptocrystalline, olivine-green crusts of kaňkite; C – zýkaite aggregate; D – stalactites of pitticite; E – erythrite aggregates; F – yellow accumulations of hydroniumjarosite and low pH waters at a bottom.

scorodite coexists with zýkaite, kaňkite, pitticite, and iron oxyhydroxides.

Scorodite was identified by the PXRD. Refined unit-cell parameters of scorodite from Radzimowice are typical for this mineral: a = 10.3144(29), b = 8.9401(31), c = 10.0331(29).

Using the EPMA, the chemical composition of scorodite from the third exploitation level was deter-

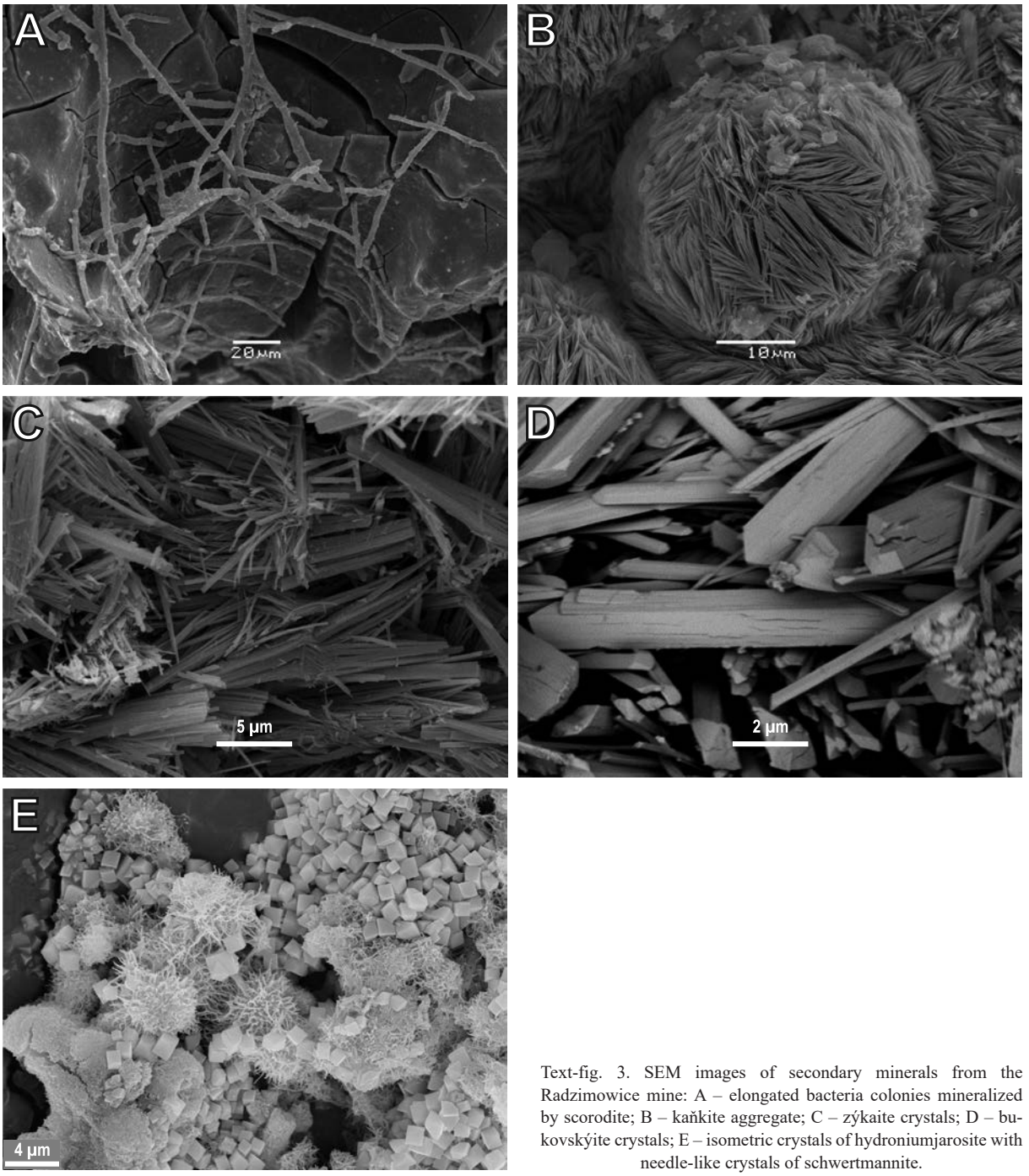

Text-fig. 3. SEM images of secondary minerals from the Radzimowice mine: A – elongated bacteria colonies mineralized by scorodite; B – kaňkite aggregate; C – zýkaite crystals; D – bukovskýite crystals; E – isometric crystals of hydroniumjarosite with needle-like crystals of schwertmannite.

mined (Table 1). The investigated scorodite is characterized by small fluctuations of the iron content (from 0.95 to 1.03 *apfu*). To a small extent, this element is replaced by aluminium (up to 0.03 *apfu*) and copper (up to 0.01 *apfu*). The content of arsenate ions at the tetrahedral site changes from 0.79 to 0.98 *apfu*. This anion is substituted by SO_4^{2-} (0.04–0.22 *apfu*) and SiO_4^{4-} (up to 0.03 *apfu*) ions.

Based on thermogravimetric studies, the content of water in the analyzed mineral was determined. The total weight loss over the temperature interval of 20–300ºC was 16.15 wt% (Text-fig. 4A). The average empirical formula of scorodite calculated based on 6 oxygen atoms per formula unit and H_2O content determined by the thermogravimetric method is: $(Fe_{0.98}Al_{0.01}Cu_{0.01})_{\Sigma=1.00}[(AsO_4)_{0.90}(SO_4)_{0.07}]_{\Sigma=0.97}\cdot 2.02H_2O$.

Analysis no.	1	2	3	4	5	6	7	8	9	10	Mean
Fe_2O_3	35.30	35.60	35.22	34.07	34.30	35.60	34.22	35.14	34.32	33.59	34.74
Al_2O_3	0.25	0.00	0.30	0.00	0.25	0.00	0.30	0.10	0.22	0.69	0.21
CuO	0.51	0.40	0.43	0.00	0.51	0.40	0.43	0.36	0.13	0.28	0.34
As_2O_5	45.35	45.31	44.74	40.74	47.35	47.93	47.02	45.62	46.75	49.77	46.06
SO_3	1.83	1.78	1.73	7.99	1.83	1.78	1.73	2.87	1.89	1.31	2.47
P_2O_5	0.14	0.00	0.10	0.00	0.14	0.00	0.10	0.16	0.11	0.00	0.07
SiO_2	0.40	0.11	0.66	0.00	0.00	0.00	0.00	0.00	0.00	0.00	0.12
H_2O	15.61*	15.61*	15.61	15.61	15.61	15.61	15.61	15.61	15.61	15.61	16.15**
Total:	99.37	98.81	98.79	98.41	99.97	101.32	99.41	99.86	99.03	101.26	100.16
atom per formula unit [*apfu*]											
Fe^{3+}	1.01	1.03	1.02	0.95	0.98	1.01	0.98	1.00	0.99	0.95	0.98
Al^{3+}	0.01	0.00	0.01	0.00	0.01	0.00	0.01	0.00	0.01	0.03	0.01
Cu^{2+}	0.01	0.01	0.01	0.00	0.01	0.01	0.01	0.01	0.00	0.01	0.01
AsO_4^{3-}	0.90	0.91	0.90	0.79	0.94	0.94	0.94	0.90	0.93	0.98	0.90
SO_4^{2-}	0.05	0.05	0.05	0.22	0.05	0.05	0.05	0.08	0.05	0.04	0.07
PO_4^{3-}	0.00	0.00	0.00	0.00	0.00	0.00	0.00	0.01	0.00	0.00	0.00
SiO_4^{4-}	0.02	0.00	0.03	0.00	0.00	0.00	0.00	0.00	0.00	0.00	0.00
H_2O	1.99	2.00	2.00	1.93	1.98	1.96	1.99	1.97	1.99	1.96	2.02

Table 1. Chemical composition of scorodite from the abandoned mine in Radzimowice (in wt%). * – content of H_2O on the basis of 3 H_2O molecules in ideal scorodite formula, ** – content of H_2O from TG analysis.

In the infrared absorption spectra several bands are observed (Text-fig. 5A). The broad absorption band with a maximum at 3374 cm^{-1} corresponds to hydroxyl stretching vibrations from H_2O molecules in scorodite. In this mineral water molecules are placed in the tunnel structure along the *c* axis and are subject to the affect of surrounding cations and anions. Interaction of H_2O molecules with the arsenate group produces two infrared active bands at around 3500 (sharp) and 2950–3050 cm^{-1} (broad) (Ondruš *et al.* 1999; Gomez *et al.* 2010; Johnson *et al.* 2020). Only one absorption band is visible on the recorded spectra. This may be because some of the arsenate ions are replaced by sulphate anions. This substitution also shifts the main absorption band (about 3500 cm^{-1}) towards lower wavenumbers (3374 cm^{-1}). A similar phenomenon was observed in the case of synthetic material with a high content of sulphate anions (Qi *at al.* 2020). The absorption band at 1631 cm^{-1} is connected with the presence of water molecules. The typical sulphate absorption bands are present at 1123 cm^{-1} (v_3), 1073 cm^{-1} (v_3) and 600 cm^{-1} (v_4) The presence of absorption bands characteristic of the sulphate group confirms its presence in the analyzed material. The absorption band at 830 cm^{-1} corresponds to the stretching and vibrations of the arsenate ions (v_3). The bending vibrations of the arsenate groups are present at 470 cm^{-1}(v_4).

Kaňkite $FeAsO_4 \cdot 3.5H_2O$

In Radzimowice kaňkite is one of the most common iron arsenates. In the abandoned mine galleries of III B exploitation level, it forms earthy, monomineral aggregates up to 40 cm in diameter. They occur directly on one of the unveiled ore veins composed of arsenopyrite and fine-grained pyrite. Kaňkite also forms cryptocrystalline, green-yellow coatings and crusts, covering the surfaces of rhyolite which contain disseminated arsenopyrite-pyrite ore (Text-fig. 2B). In the natural humidity state kaňkite is soft and plastic and has a brilliant green-yellow colour. At very high magnifications thin-plate crystals of the mineral may be observed (Text-fig. 3B). In underground mining pits kaňkite coexists with scorodite, zýkaite, and pitticite. Near kaňkite accumulations of hydroniumjarosite and Fe oxyhydroxides precipitate.

Refined unit-cell parameters of kaňkite from Radzimowice are within the typical range for this mineral: a = 18.715(36), b = 17.471(34), c = 7.638(18), β = 92.825(39) (Čech *et al.* 1976).

Quantitative chemical analysis of kaňkite is present in Table 2. The amount of iron in kaňkite varies in a small range from 0.93 to 0.99 *apfu*. Only small amounts of Al (to 0.03 *apfu*) are associated with it. At the tetrahedral position AsO_4^{3-} ion (content from 0.89 to 0.98 *apfu*) is partially replaced by SO_4^{2-} (0.01–0.21 *apfu*) and PO_4^{3-} (up to 0.13 *apfu*) ions. A similar level of substitution of arsenate ion by sulphate ion was documented for kaňkite from the area of the Czech Republic (Kocourková *et al.* 2008) and the weathering zone of the Suzukura deposit in Japan (Kato *et al.* 1984).

The water content in kaňkite was estimated by the TG method. The process of water release is two-stage

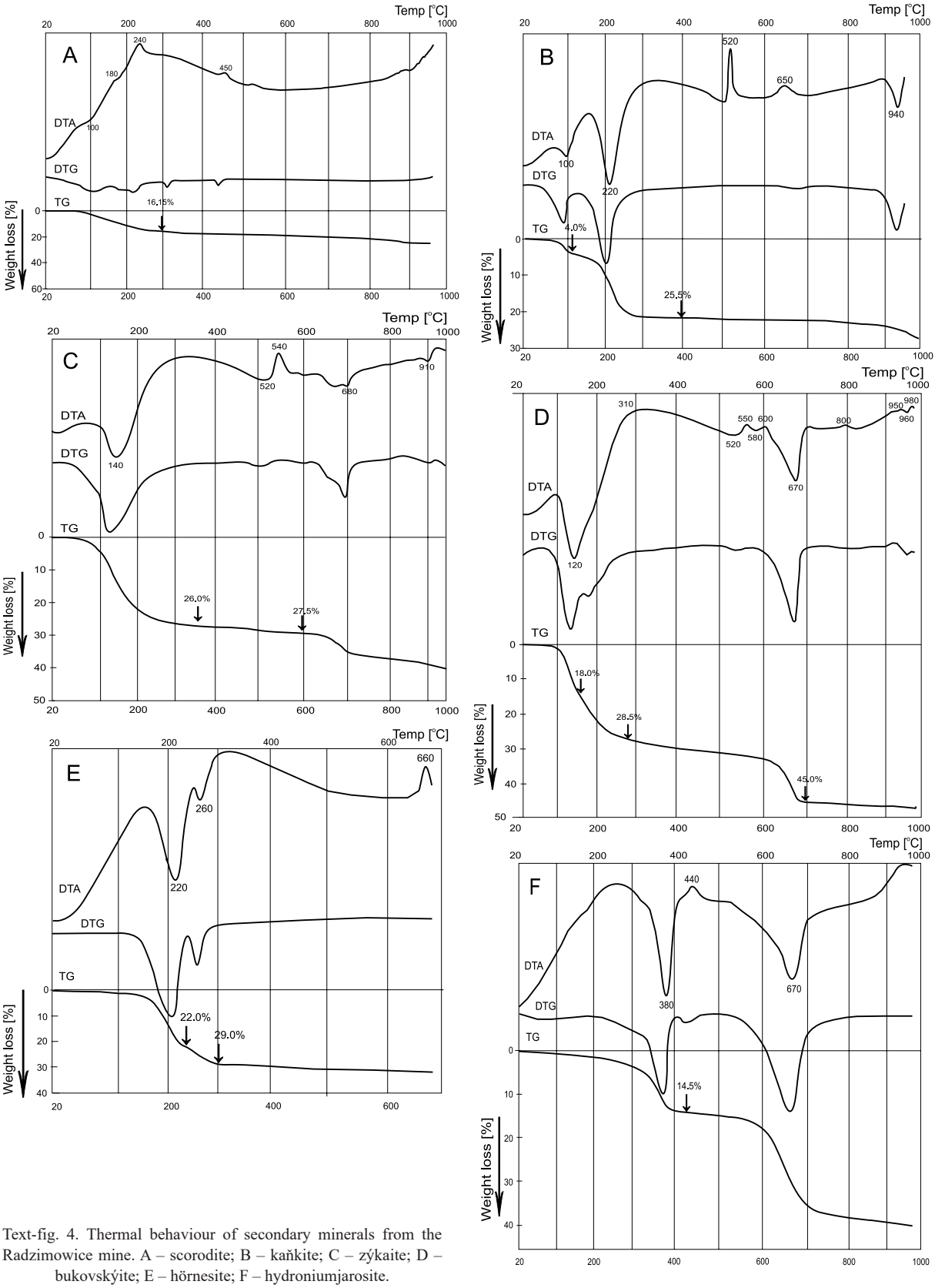

Text-fig. 4. Thermal behaviour of secondary minerals from the Radzimowice mine. A – scorodite; B – kaňkite; C – zýkaite; D – bukovskýite; E – hörnesite; F – hydroniumjarosite.

Analysis no	1	2	3	4	5	6	7	8	9	10	Mean
Fe_2O_3	30.17	29.99	29.99	29.76	29.13	31.25	31.10	30.64	30.71	30.85	30.36
Al_2O_3	0.09	0.00	0.52	0.20	0.30	0.19	0.09	0.10	0.60	0.00	0.21
As_2O_5	42.31	32.75	43.81	43.51	42.24	40.85	41.91	41.65	40.76	43.92	41.37
SO_3	2.60	6.60	2.24	2.19	2.38	3.29	2.18	2.39	3.36	0.43	2.77
P_2O_5	0.00	3.66	0.08	0.06	0.12	0.37	0.40	0.33	0.35	0.13	0.55
SiO_2	0.03	bdl	0.04	bdl	0.07	0.03	0.03	0.03	0.07	bdl	0.03
H_2O	24.46*	24.46*	24.46*	24.46*	24.46*	24.46*	24.46*	24.46*	24.46*	24.46*	25.50**
Total:	100.24	99.05	102.20	100.88	98.99	101.49	100.86	100.15	101.43	99.89	100.79
atom per formula unit [*apfu*]											
Fe^{3+}	0.96	0.93	0.94	0.95	0.93	0.98	0.99	0.98	0.97	0.99	0.94
Al^{3+}	0.00	0.00	0.03	0.01	0.02	0.01	0.00	0.00	0.03	0.00	0.01
AsO_4^{3-}	0.94	0.71	0.96	0.96	0.94	0.89	0.92	0.92	0.89	0.98	0.89
SO_4^{2-}	0.08	0.21	0.07	0.07	0.08	0.10	0.07	0.08	0.11	0.01	0.09
PO_4^{3-}	0.00	0.13	0.00	0.00	0.00	0.01	0.01	0.01	0.01	0.00	0.02
SiO_4^{4-}	0.00	0.00	0.00	0.00	0.00	0.00	0.00	0.00	0.00	0.00	0.00
H_2O	3.45	3.38	3.41	3.45	3.47	3.42	3.44	3.45	3.42	3.49	3.51

Table 2. Chemical composition of kaňkite from the abandoned mine in Radzimowice (in wt%). * – content of H_2O on the basis of 3.5 H_2O molecules in ideal kaňkite formula, ** – content of H_2O from TG analysis, bdl – below detection limit.

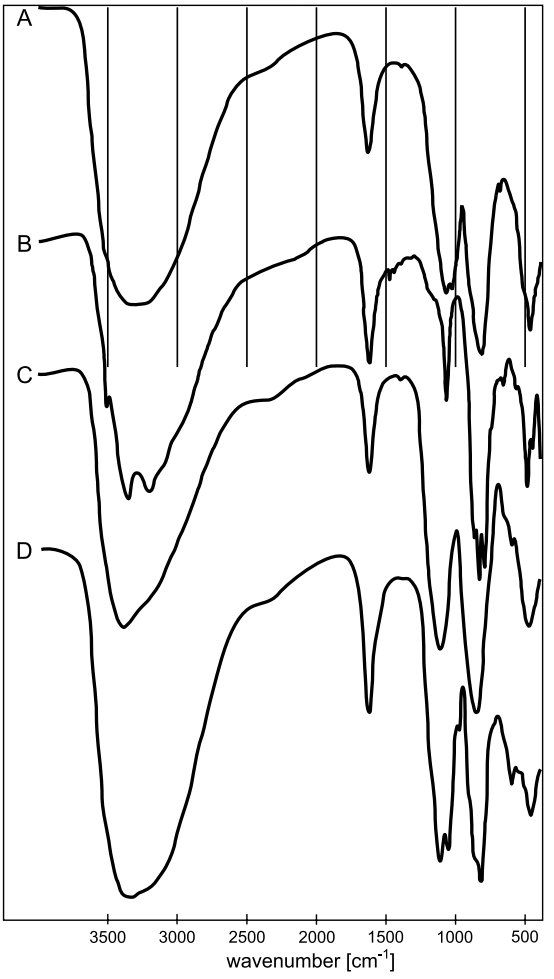

Text-fig. 5. The IR spectra of secondary arsenic minerals from the Radzimowice mine (A – scorodite; B – kaňkite; C – zýkaite; D – bukovskýite).

(Text-fig. 4B), which may point to a different degree of the crystallization water binding in its structure (Kato *et al*. 1984). The total mass loss of the sample equals 25.50 wt%. The empirical formula of kaňkite from the second mine level (based on 7.5 oxygen atoms per formula unit and H_2O content determined by the thermogravimetric method) is $(Fe_{0.94}Al_{0.01})_{\Sigma=0.95}[(AsO_4)_{0.89}(SO_4)_{0.09}(PO_4)_{0.02}]_{\Sigma=1.00}\cdot 3.51H_2O$.

In the obtained IR spectrum for kaňkite few characteristic absorption bands are seen (Text-fig. 5B). Bands centered at 3518, 3364 and 3210 cm^{-1} are due to H-O stretching vibrations in the molecules of crystallization water. The presence of three absorption bands in the 3500–3200 cm^{-1} range may indicate the occurrence of three non-equivalent positions of H_2O molecules in the structure of kaňkite under the scope. It is noteworthy that such subbands have not been observed by other researches (Kato *et al*. 1984; Frost *et al*. 2015). The group of absorption bands at 1485, 1455, 1409 and 1329 cm^{-1} come from δ (As-OH) modes, while bands at 873, 840, and 799 cm^{-1} come from ν_3 symmetry deformation of AsO_4^{3-}. The presence of sulphate ion replacing arsenate ion is confirmed by the presence of a 1074 cm^{-1} band due to ν_3 vibrations.

Zýkaite $Fe_4(AsO_4)_3(SO_4)(OH)\cdot 15H_2O$

In the abandoned mine galleries of the III B exploitation level of Radzimowice mine, zýkaite occurs in the form of white, porous, rounded aggregates up to 4 cm in size (Text-fig. 2C). They grow on the surface of rhyolites containing weathering arsenic ores or at the bottom of mining galleries between rock frag-

Analysis no.	1	2	3	4	5	6	7	8	9	10	Mean
Fe_2O_3	30.52	30.44	30.29	30.61	30.06	30.65	31.13	31.09	31.10	31.22	30.71
Al_2O_3	0.48	0.46	0.50	0.45	0.49	0.32	0.00	0.00	0.00	0.00	0.27
K_2O	0.42	0.29	0.51	0.17	0.35	0.20	0.37	0.29	0.42	0.19	0.32
As_2O_5	33.95	34.02	34.05	36.20	35.88	34.12	34.31	33.75	33.75	33.87	34.39
SO_3	6.94	7.33	6.78	4.79	6.30	7.71	7.77	7.50	7.83	7.91	7.09
H_2O	27.50*	27.50*	27.50*	27.50*	27.50*	27.50*	27.50*	27.50*	27.50*	27.50*	27.50**
Total:	99.81	100.04	99.63	99.72	100.59	100.50	101.08	100.13	100.60	100.69	100.28
atom per formula unit [*apfu*]											
Fe^{3+}	3.94	3.76	3.91	3.99	3.86	3.90	3.96	3.98	3.97	3.98	3.91
Al^{3+}	0.10	0.09	0.10	0.09	0.10	0.06	0.00	0.00	0.00	0.00	0.05
K^+	0.09	0.06	0.11	0.04	0.08	0.04	0.08	0.06	0.09	0.04	0.07
AsO_4^{3-}	3.04	2.92	3.06	3.28	3.20	3.02	3.03	3.00	2.99	3.00	3.04
SO_4^{2-}	0.89	0.90	0.87	0.62	0.81	0.98	0.98	0.96	1.00	1.01	0.90
OH^{-***}	1.28	1.04	1.24	1.20	0.73	0.93	0.89	1.08	1.03	0.97	1.04
H_2O	14.86	15.09	14.31	15.03	15.40	15.08	14.96	14.82	14.98	14.93	14.91

Table 3. Chemical composition of zýkaite from the abandoned mine in Radzimowice (in wt%). * – content of H_2O on the basis of ideal zýkaite formula, ** – content of H_2O from TG analysis, *** – content of OH^- was calculated from charge balance.

ments. In the natural humidity state, the aggregates are plastic and become brittle when dried. In the BSE image needle-like crystals, up to 20 μm in length are observed (Text-fig. 3C). Zýkaite from mine pits is associated with small amounts of kaňkite, scorodite, hydroniumjarosite and pitticite.

Zýkiate was identified by X-ray powder diffraction. Refined unit-cell parameters of zýkaite from Radzimowice are typical for this mineral: a = 20.87(15), b = 7.043(54), c = 36.89(25).

The chemical composition of zýkaite was determined using the electron microprobe (Table 3). Iron content varies from 3.76 to 3.99 *apfu*. This element is replaced slightly by aluminium (up to 0.10 *apfu*) and potassium (from 0.04 to 0.11 *apfu*). The amount of arsenate ion changes from 2.92 to 3.28 *apfu*. It is associated with SO_4^{2-} (from 0.62 to 1.01 *apfu*).

In the obtained DTA curve four endothermic effects may be seen (Text-fig. 4C). The first one has a maximum at 140ºC and is related to crystallization water loss. This reaction corresponds to a weight loss of 26.0 % of the total sample mass. The next endothermic effect, with a maximum at 520ºC, is attributable to the release of the hydroxyl groups.

The empirical formula of zýkaite, based on 32 oxygen atoms and considering H_2O amount from TG analysis is $(Fe_{3.91}Al_{0.05}K_{0.07})_{\Sigma=4.03}(AsO_4)_{3.04}(SO_4)_{0.90}(OH)_{1.04}\cdot 14.91H_2O$.

The IR spectrum of zýkaite from Radzimowice (Text-fig. 5C) is similar to that obtained for the holotype material (Čech *et al.* 1978). The broad band with a maximum at 3387 cm^{-1} is due to O-H stretching. The band at 1667 cm^{-1} comes from H-O-H bending in water molecules. Absorption bands at 1116 and 1075 cm^{-1} come from $\nu_3(SO_4^{2-})$, and the band at 599 cm^{-1} came from ν_4 of the same anion. The ν_3 arsenate ion deformation vibrations give the band at 850 cm^{-1}, and the ν_4 ones the band at 479 cm^{-1}.

Bukovskýite $Fe_2(AsO_4)(SO_4)(OH)\cdot 7H_2O$

The occurrence of bukovskýite was established only at the II exploitation level of the mine in Radzimowice. The mineral occurs as light yellow earthy aggregates up to several millimetres in diameter. They grow on the surface of rhyolites containing weathering arsenopyrite. At high magnifications thin needle-like crystals of the mineral are observed, reaching 10 μm in length (Text-fig. 3D). Cracks parallel to crystal elongation are often seen on their surface. They are probably caused by the loss of water. Bukovskýite coexists with melanterite, amorphous Fe oxyhydroxides and small amounts of hydroniumjarosite.

The refined unit-cell parameters of bukovskýite from Radzimowice are typical for this mineral: a = 10.7218(41), b = 14.112(12), c = 10.2432(44), α = 93.391(29), β = 115.901(22), γ = 90.258(33) (Novák *et al*. 1967).

The chemical composition of bukovskýite from Radzimowice is close to the holotype material from Kaňk in the Czech Republic (Table 4). The amount of arsenate and sulphate ions varies slightly (0.96–1.07 *apfu* and 0.85–0,94 *apfu* respectively).

The DTA curve of bukovskýite from Radzimowice shows a few endothermic effects (Text-fig. 4D). The first of them, centred at 120°C, is due to crystallization water and hydroxyl groups loss. This process is two-stage, which is reflected in the shape of the DTG

Analysis no.	1	2	3	4	5	6	7	8	9	10	Mean
Fe_2O_3	34.10	34.38	35.12	33.88	33.48	34.42	35.29	34.60	34.79	33.71	34.38
As_2O_5	24.41	23.30	23.95	24.68	25.15	24.58	23.50	24.61	22.57	24.92	24.17
SO_3	14.50	13.71	14.04	14.21	14.47	14.12	14.27	14.38	15.33	13.98	14.30
P_2O_5	0.23	0.22	0.30	0.21	0.21	0.36	0.31	0.21	0.30	0.36	0.27
H_2O	27.59*	27.59*	27.59*	27.59*	27.59*	27.59	27.59*	27.59*	27.59*	27.59*	27.50**
Total:	100.83	99.20	101.00	100.57	100.90	101.07	100.96	101.39	100.58	100.56	100.62
atom per formula unit [*apfu*]											
Fe^{3+}	2.10	2.15	2.17	2.09	2.06	2.12	2.17	2.12	2.14	2.08	2.12
AsO_4^{3-}	1.04	1.01	1.03	1.06	1.07	1.05	1.01	1.05	0.96	1.07	1.04
SO_4^{2-}	0.89	0.85	0.86	0.88	0.89	0.87	0.88	0.88	0.94	0.86	0.88
PO_4^{3-}	0.02	0.02	0.02	0.01	0.01	0.02	0.02	0.01	0.02	0.02	0.02
OH^{-***}	1.34	1.66	1.63	1.31	1.13	1.39	1.69	1.42	1.58	1.24	1.44
H_2O	6.86	6.82	6.72	6.90	6.95	6.83	6.69	6.80	6.72	6.93	6.81

Table 4. Chemical composition of bukovskýite from the abandoned mine in Radzimowice (in wt%). * – content of H_2O on the basis of ideal bukovskýite formula, ** – content of H_2O from TG analysis, *** – content of OH^- was calculated from charge balance.

curve. This reaction corresponds to a weight loss of 28.5 wt%.

The empirical formula of bukovskýite, based on 16 oxygen atoms and considering the H_2O amount from the TG analysis is $Fe_{2.12}(AsO_4)_{1.04}(SO_4)_{0.88}(PO_4)_{0.02}(OH)_{1.44}\cdot 6.810H_2O$. The calculated empirical formula is in good correspondence to that proposed by Novák *et al.* (1967) and differs from the formula developed by Majzlan *et al.* (2012) in having a lesser amount of crystallization water. This may suggest, that the number of H_2O molecules in bukovskýite changes from 7 to 9 and depends on the humidity of the crystallization environment.

In the infrared absorption spectra several bands are observed (Text-fig. 5D). The broad absorption band with a maximum at 3363 cm^{-1} corresponds to the stretching vibrations of the O-H bond. The absorption band at 1633 cm^{-1} is connected with the presence of water molecules. The typical sulphate absorption bands are present at 1121 cm^{-1} (ν_3), 1062 cm^{-1} (ν_3), 983 cm^{-1} (ν_1), 603 cm^{-1} (ν_4). The absorption band at 832 cm^{-1} corresponds to the stretching and vibrations of the arsenate ions (ν_3). The bending vibrations of the arsenate groups are present at 472 cm^{-1}(ν_4). The position of the absorption bands is close to the position recorded for the holotypic material from Kaňk near Kutna Hora (Novák *et al.* 1967; Loun *et al.* 2011).

Pitticite

Pitticite is an amorphous arsenosulphate of iron and has a labile chemical composition (Dunn 1982; Filippi *et al.* 2004; Salzsauler *et al.* 2005; Gieré *et al.* 2003; Frost *et al.* 2011; Frost *et al.* 2012). The largest accumulations of this phase occur at the III B exploitation level of the Radzimowice mine. The phase mainly forms stalactites and stalagmites up to 20 cm in length (Text-fig. 2D). Its colour changes from light beige through seal to black. Pitticite is associated with scorodite, amorphous iron oxyhydroxides, zýkaite, kaňkite and hydroniumjarosite. Diffraction analyses confirmed the amorphous nature of pitticite from Radzimowice.

This mineral phase is characterized by a very high lability of chemical composition (Table 5). The iron content changes in a very vast range from 29.81 to 70.51 wt% Fe_2O_3. Sometimes the element is associated with small amounts of aluminium (up to 0.74 wt% Al_2O_3), manganese (up to 0.10 wt% MnO), copper (up to 0.13 wt% CuO), calcium (up to 0.09 wt% CaO), sodium (up to 0.14 wt% Na_2O), and potassium (up to 0.45 wt% K_2O). The arsenic content

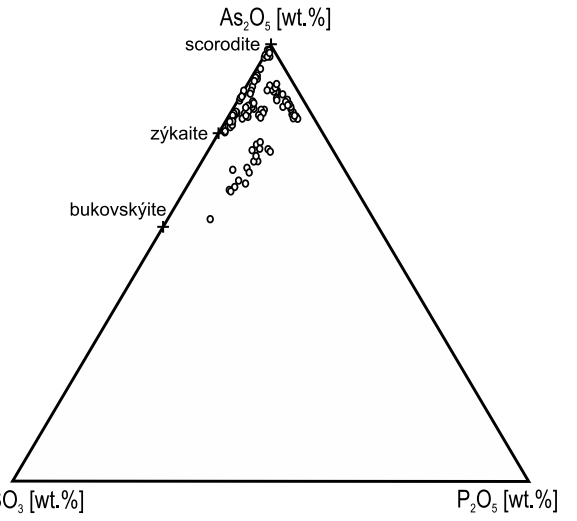

Text-fig. 6. A triangular plot of the chemical compositions of the pitticite from the underground mining excavations in Radzimowice.

Analysis no.	1	2	3	4	5	6	7	8	9	10
Fe_2O_3	38.62	34.60	36.47	37.48	36.88	37.39	37.78	30.17	31.08	29.81
Al_2O_3	0.10	0.74	bdl	bdl	bdl	bdl	bdl	bdl	bdl	bdl
MnO	bdl	bdl	bdl	bdl	bdl	bdl	0.00	0.00	bdl	bdl
CuO	bdl	bdl	bdl	bdl	bdl	bdl	bdl	bdl	bdl	bdl
Na_2O	bdl	bdl	bdl	bdl	bdl	0.00	0.00	0.13	0.00	0.00
K_2O	0.00	0.00	0.07	0.00	0.00	0.09	0.18	0.00	0.06	0.00
CaO	0.00	0.00	0.00	0.08	0.00	0.00	0.07	0.00	0.00	0.00
As_2O_5	53.40	53.57	45.50	45.91	46.46	44.82	42.65	43.34	44.48	43.50
SO_3	0.65	0.72	3.17	3.07	2.86	2.00	1.80	1.43	1.58	1.49
P_2O_5	0.00	0.00	0.34	0.45	0.42	3.01	3.03	5.01	4.86	4.81
SiO_2	0.00	0.00	0.00	0.00	0.00	0.00	0.00	0.00	0.00	0.00
Total:	92.78	89.63	85.55	86.99	86.62	87.30	85.51	80.09	82.06	79.61
Analysis no.	11	12	13	14	15	16	17	18	19	20
Fe_2O_3	38.18	38.66	39.06	34.3	35.19	35.93	34.52	36.77	64.56	70.51
Al_2O_3	0.00	0.00	0.00	0.00	0.00	0.00	0.08	0.00	0.00	0.00
MnO	0.07	0.00	0.00	0.10	0.00	bdl	bdl	bdl	0.00	0.00
CuO	bdl	bdl	0.00	0.00	0.00	0.00	0.13	0.00	0.00	0.00
Na_2O	bdl	bdl	0.00	0.08	0.14	0.00	0.00	0.11	0.12	0.00
K_2O	0.00	0.00	0.00	0.00	0.45	0.00	0.00	0.10	0.00	0.00
CaO	0.09	0.00	0.07	0.00	0.00	0.00	0.00	0.06	0.00	0.00
As_2O_5	38.58	38.25	40.06	32.53	32.32	30.84	32.17	39.93	19.14	16.29
SO_3	7.64	7.80	4.84	5.23	5.14	4.02	3.89	4.77	5.07	5.97
P_2O_5	0.33	0.34	2.88	4.76	5.04	0.00	0.07	2.70	2.71	2.11
SiO_2	0.00	0.00	0.00	0.00	0.00	0.00	0.06	0.00	0.25	0.33
Total:	84.89	85.05	86.91	77.00	78.28	70.79	70.91	84.44	91.85	95.21

Table 5. Representative compositions of different pitticite aggregates from the abandoned mine in Radzimowice (in wt%).

in aggregates varies from 16.29 to 53.57 wt% As_2O_5. Arsenic is associated with variable amounts of sulphur (from 0.65 to 7.80 wt% SO_3) and phosphorus (up to 5.04 wt% P_2O_5) (Text-fig. 6). It is important to note, that the largest amounts of phosphorus were determined in pitticite dripstones related to bacteria colonies. Such a large variability of the iron and arsenic content indicates that some of the pitticite aggregates belong to amorphous iron arsenate with a composition similar to the scorodite (analysis no 1–10) . This type of pitticitite may be a precursor of the crystalline iron arsenate – scorodite. Another aggregate corresponds to the amorphous iron sulphate-arsenate in its composition (analysis no 11–18). The chemical composition of some pittycite accumulations corresponds to iron oxyhydroxides with absorbed arsenate and sulphate ions (analysis no 19–20).

Erythrite $Co_2(AsO_4)\cdot 8H_2O$ – annabergite $Ni_2(AsO_4)\cdot 8H_2O$ – hörnesite $Mg_2(AsO_4)\cdot 8H_2O$ series

Minerals of this series appear only in the third level of the mine. Erythrite forms very fine spherical aggregates, ≤2 mm in diameter, comprising thin crystals. The colour of the clusters varies from purple to light pink (Text-fig. 2E). Erythrite grows on the surface of the weathered ore veins composed of Co-rich arsenopyrite, cobaltite and dolomite.

Due to the small size of erythrite aggregates, no X-ray diffraction studies were performed. The chemical composition of the purple erythrite shows extensive substitutions in cation sites (Table 6). In addition to the Co content (1.68 to 1.93 *apfu*) substantial contents of Ni (from 0.68 to 0.72 *apfu*), Mg (from 0.28 to 0.35 *apfu*) and Ca (from 0.06 to 0.12 *apfu*) occurred in the purple erythrite variety. Other elements, such as Zn, Mn Fe, and Cu, do not play a significant role. This type of erythrite belongs to the erythrite-annabergite-hörnesite series. The empiric formula of the purple erythrite variety is $(Co_{1.89}Ni_{0.70}Mg_{0.31}Ca_{0.08}Mn_{0.03}Zn_{0.01}Fe_{0.01})_{\Sigma=2.72}(AsO_4)_{2.0}\cdot 7.94H_2O$. This formula was calculated on the basis of 16 oxygen atoms, using an average of 5 spot analyses.

The compositional study of light pink colored erythrite proved a rather extensive substitution in the cation site (Table 6). The dominant Co^{2+} cation is replaced by Mg^{2+} (from 0.71 to 0.75 *apfu*), Zn^{2+} (from 0.28 to 0.34 *apfu*), Mn^{2+} (from 0.19 to 0.20 *apfu*) and Cu^{2+} (from 0.09 to 0.16 *apfu*). This variety of erythrite is poor in nickel and belongs to several

Analysis no.	1	2	3	4	5	6	7	8	9	10
	Purple erythrite					Light pink erythrite				
CoO	24.00	24.26	23.85	24.14	23.14	21.23	21.79	22.14	21.00	20.31
NiO	8.93	8.57	8.75	9.01	8.69	0.16	0.27	0.24	0.24	0.16
MgO	2.36	2.11	2.08	1.87	2.15	4.90	4.87	4.97	5.06	5.12
ZnO	0.11	0.19	0.19	0.15	0.12	4.74	4.47	3.87	3.83	4.55
MnO	0.28	0.32	0.30	0.51	0.37	2.31	2.37	2.43	2.27	2.25
CuO	bdl	bdl	bdl	bdl	bdl	1.35	1.49	1.26	1.81	2.18
FeO	0.00	0.23	0.12	0.14	0.22	0.15	0.05	0.00	0.30	0.26
CaO	0.58	0.62	0.88	0.68	1.09	0.09	0.08	0.00	0.11	0.12
As_2O_5	38.78	38.75	38.87	38.77	38.52	38.95	39.12	38.95	39.23	39.41
SiO_2	0.00	0.00	0.00	0.10	0.09	0.10	0.13	0.10	0.11	0.12
H_2O	24.07	24.07	24.07	24.07	24.07	24.07	24.07	24.07	24.07	24.07
Total:	99.11	99.12	99.11	99.44	98.46	98.05	98.70	98.03	98.03	98.54
atom per formula unit [*apfu*]										
Co^{2+}	1.90	1.93	1.89	1.91	1.84	1.68	1.71	1.75	1.65	1.60
Ni^{2+}	0.71	0.68	0.70	0.72	0.69	0.01	0.02	0.02	0.02	0.01
Mg^{2+}	0.35	0.31	0.31	0.28	0.32	0.72	0.71	0.73	0.74	0.75
Zn^{2+}	0.01	0.01	0.01	0.01	0.01	0.34	0.32	0.28	0.28	0.33
Mn^{2+}	0.02	0.03	0.03	0.04	0.03	0.19	0.20	0.20	0.19	0.19
Cu^{2+}	0.00	0.00	0.00	0.00	0.00	0.10	0.11	0.09	0.13	0.16
Fe^{2+}	0.00	0.02	0.01	0.01	0.02	0.01	0.00	0.00	0.02	0.02
Ca^{2+}	0.06	0.07	0.09	0.07	0.12	0.01	0.01	0.00	0.01	0.01
AsO_4^{3-}	2.00	2.00	2.01	2.00	2.00	2.00	2.01	2.00	2.02	2.02
SiO_4^{4-}	0.00	0.00	0.00	0.01	0.01	0.01	0.01	0.01	0.01	0.01
H_2O	7.94	7.94	7.94	7.93	7.96	7.90	7.87	7.90	7.89	7.86

Table 6. Representative compositions of erythrite from the abandoned mine in Radzimowice (in wt%). * – content of H_2O on the basis of ideal erythrite formula, bdl – below detection limit

isomorphic series (erythrite-hörnesite-köttigite-manganohörnesite-babánekite). The empiric formula of light pink erythrite calculated on the basis of 16 oxygen atoms and from average of 5 spot analyses is: $(Co_{1.68}Mg_{0.73}Zn_{0.31}Mn_{0.19}Cu_{0.12}Ni_{0.02}Ca_{0.01}Fe_{0.01})_{\Sigma 3.07}$ $[(AsO_4)_{2.01}(SiO_4)_{0.01}]_{\Sigma=2.00}\cdot 7.88H_2O$.

Small, spherical hörnesite aggregates, up to 0.3 cm in diameter, occur on the third level of the mine. This mineral grows on the surface of the dolomite vein that crosses quartz-sericite-graphite schists with disseminated arsenopyrite mineralization. Hörnesite was identified by X-ray powder diffraction. The refined unit-cell parameters of hörnesite from Radzimowice are typical for this mineral: a = 10.2611(77), b = 13.4379(48), c = 4.7434(28), β = 104.983(63).

The dominating cation in the octahedral site of hörnesite is Mg^{2+} (2.54–2.70 *apfu*), while the subordinate is Co^{2+} (0.21–0.30 *apfu*) accompanied by minor Mn^{2+}, Ni^{2+}, Zn^{2+}, Ca^{2+}, and Fe^{2+} cations (Table 7).

The content of water in the analyzed hörnesite was estimated by the TG method (Text-fig. 4E). The mineral dehydration process occurs in two stages, which correspond to two endothermic effects with a maximum of 220 and 260 ºC respectively. The total weight loss associated with water loss is 29 wt%. The endotherm effect with a maximum at 660 ºC is related to the recrystallization of the anhydrous phase.

The chemical composition of hörnesite (average of five spot analyses, water content determined by thermal analysis), recalculated based on 16 oxygen atoms, yields the following formula: $(Mg_{2.64}Co_{0.25}Mn_{0.04}Fe_{0.02}Ca_{0.02}Zn_{0.01}Cu_{0.01})_{\Sigma=2.99}$ $(AsO_4)_{1.99}\cdot 8{,}04H_2O$.

Ferrihydrite $Fe^{3+}{}_{10}O_{14}(OH)_2$

This phase occurs in the form of rusty dripstones associated with zones of intensive oxidation of ore minerals. In old mine galleries, ferrihydrite aggregates may reach 2 metres in thickness (Parafiniuk and Siuda 2006). The mineral is accompanied by variable amounts of goethite, scorodite, and amorphous iron arsenates. Ferrihydrite was identified by PXRD.

Gypsum $CaSO_4\cdot 2H_2O$

Gypsum occurs commonly in underground mine galleries, especially in the zones of oxidation of ore mineralization as tabular or thin needle crystals up to

Analysis no.	1	2	3	4	5	Mean
MgO	20.30	21.05	21.78	21.92	21.56	21.32
CoO	4.48	3.97	3.55	3.15	3.38	3.71
ZnO	0.28	0.40	0.11	0.00	0.17	0.19
NiO	0.00	0.25	0.00	0.11	0.00	0.07
MnO	0.62	0.59	0.45	0.41	0.54	0.52
FeO	0.24	0.24	0.22	0.26	0.23	0.24
CuO	0.20	0.12	0.17	0.10	0.00	0.12
CaO	0.20	0.20	0.18	0.13	0.23	0.19
As_2O_5	44.64	46.20	46.08	46.24	45.87	45.81
H_2O	29.12*	29.12*	29.12*	29.12*	29.12*	29.00**
Total:	100.08	102.13	101.66	101.44	101.10	101.16
atom per formula unit [*apfu*]						
Mg^{2+}	2.54	2.59	2.68	2.70	2.67	2.64
Co^{2+}	0.30	0.26	0.24	0.21	0.22	0.25
Zn^{2+}	0.02	0.02	0.01	0.00	0.01	0.01
Ni^{2+}	0.00	0.02	0.00	0.01	0.00	0.00
Mn^{2+}	0.04	0.04	0.03	0.03	0.04	0.04
Fe^{2+}	0.02	0.02	0.02	0.02	0.02	0.02
Cu^{2+}	0.01	0.01	0.01	0.01	0.00	0.01
Ca^{2+}	0.02	0.02	0.02	0.01	0.02	0.02
AsO_4^{3-}	1.96	2.00	1.99	2.00	1.99	1.99
H_2O	8.15	8.03	8.03	8.03	8.05	8.04

Table 7. Chemical composition of hörnesite from the abandoned mine in Radzimowice (in wt%). * – content of H_2O on the basis of ideal hörnesite formula, ** – content of H_2O from TG analysis.

3 cm in length. Gypsum coexists with Fe oxyhydroxides, iron arsenates, and hydroniumjarosite.

Hydroniumjarosite $(H_3O)Fe_3[(OH)_6|(SO_4)_2]$ – jarosite $KFe_3[(OH)_6|(SO_4)_2]$) solid solution

Minerals of this solution series occur as light yellow argillaceous covers comprising tiny crystals up to 1.5 μm. They usually cover the surfaces of mine galleries that were dripped by acid mine waters. Sometimes also larger aggregates of this mineral are met, and they reach a few centimetres in diameter. They are often associated with gelatinous microorganism colonies or form accumulations at the galleries' bottom in places where low pH waters stagnate (Text-fig. 2F). The thickness of these accumulations may reach 0.5 m. The aggregates of hydroniumjarosite-jarosite are usually monomineral, without traces of other supergene minerals. Sometimes the mineral is accompanied by variable amounts of schwertmannite (Text-fig. 3E).

Hydroniumjarosite was identified by PXRD. The refined unit-cell parameters of hydroniumjarosite from Radzimowice are typical for this mineral: a = 7.31485(80), c = 17.1139(25).

The chemical composition was determined with the use of an electron microprobe (Table 8). In the analysed mineral, significant variations in the K^+ ion content are observed (from 0.31 to 0.56 *apfu*). Potassium deficiency is compensated by hydronium ions. The tetrahedral site is mainly occupied by sulphate ions (from 1.93 to 2.04 *apfu*). It is replaced to a small extent by arsenic (up to 0.11 *apfu*) and phosphorus (up to 0.04 *apfu*).

Few thermal effects may be observed in the DTA curve. (Text-fig. 4F). The first endothermic effect, with a maximum at 380ºC, is due to hydronium water loss. It is important to note, that this reaction takes place at a slightly higher temperature than in the case of pure hydroniumjarosite. It is characteristic for the hydroniumjarosite-jarosite series (Kubisz 1971). The process of release of hydroxyl groups is marked by a light deflection of the DTA curve, with a maximum at 420 ºC. Determined on the basis of thermogravimetric research the amount of water in jarosite under scope equals ca. 14.5 wt%. The following empirical formula was calculated from the average of 10 spot analyses and thermogravimetric data based on 15 oxygen atoms: $(H_3O_{0.55}K_{0.45})_{\Sigma=1.00}(Fe_{3.09}Al_{0.02})_{\Sigma=3.11}[(SO_4)_{1.98}(AsO_4)_{0.03}(PO_4)_{0.02}]_{\Sigma=2.03}(OH)_{6.45}$.

Melanterite $FeSO_4 \cdot 7H_2O$

At the second exploitation level of the Radzimowice mine melanterite is present as greenish aggregates forming crusts on weathering pyrite-arsenopy-

Analysis no.	1	2	3	4	5	6	7	8	9	10	Mean
K_2O	4.45	4.18	3.81	3.92	4.43	5.24	3.66	2.96	4.50	4.60	4.17
Fe_2O_3	49.56	48.53	49.45	49.10	49.45	48.30	50.23	48.37	48.13	48.58	48.97
Al_2O_3	0.22	0.00	1.75	0.11	0.34	0.00	0.00	0.00	0.00	0.00	0.24
SO_3	31.53	32.33	31.16	32.51	31.36	31.68	31.99	30.92	30.62	30.66	31.48
As_2O_5	0.79	0.00	0.00	0.00	0.00	0.00	0.00	2.10	2.39	2.14	0.74
P_2O_5	0.24	0.00	0.00	0.00	0.58	0.36	0.46	0.23	0.28	0.34	0.25
H_2O	13.21*	14.97*	13.83*	14.37*	13.84*	14.42*	13.66*	15.41*	14.09*	13.69*	14.50**
Total:	100.00	100.00	100.00	100.00	100.00	100.00	100.00	100.00	100.00	100.00	100.35
atom per formula unit [*apfu*]											
K^+	0.48	0.44	0.41	0.42	0.48	0.56	0.39	0.31	0.49	0.50	0.45
Fe^{3+}	3.18	3.04	3.14	3.09	3.15	3.06	3.19	3.02	3.07	3.12	3.09
Al^{3+}	0.02	0.00	0.17	0.01	0.03	0.00	0.00	0.00	0.00	0.00	0.02
SO_4^{2-}	2.02	2.02	1.97	2.04	1.99	2.00	2.03	1.93	1.95	1.96	1.98
AsO_4^{3-}	0.04	0.00	0.00	0.00	0.00	0.00	0.00	0.09	0.11	0.10	0.03
PO_4^{3-}	0.02	0.00	0.00	0.00	0.04	0.03	0.03	0.02	0.02	0.02	0.02
H_3O^{+***}	0.52	0.56	0.59	0.58	0.52	0.44	0.61	0.69	0.51	0.50	0.55
OH^-	5.96	6.63	6.02	6.28	6.25	6.78	5.86	6.46	6.44	6.28	6.45

Table 8. Chemical composition of hydroniumjarosite from the abandoned mine in Radzimowice (in wt%). * – water content as a difference up to 100%, ** – content of H_2O from TG analysis, *** – the amount of hydronium ion as 1 – potassium content.

rite intergrowths (Parafiniuk *et al.* 2016). They are built of strongly bent hair-like crystals, up to 1.5 cm in length. Melanterite is associated with bukovskýite and small amounts of hydroniumjarosite.

Schwertmannite
$Fe_{16}^{3+}(OH,SO_4)_{12–13}O_{16}\cdot 10\text{-}12H_2O$

In the abandoned mine galleries schwertmannite occurs in relatively narrow zones related to the weathering of polymetallic veins rich in pyrite and arsenopyrite (Parafiniuk and Siuda 2006). It occurs as unconsolidated stalactites and stalagmites leaching tens of centimetres in length. Accumulations of schwertmannite are built of characteristic spherical aggregates comprising thin needle-like crystals. Schwertmannite coexists with hydroniumjarosite and pitticite (Text-fig. 3E).

PARAGENESES OF IRON ARSENATES AND THE CONDITIONS OF THEIR FORMATION

Based on the current research three main assemblages of secondary arsenic minerals can be assigned. Their variable phase composition is related to the variation of geochemical conditions in which these parageneses arise.

The first assemblage occurs only at the II exploitation level (about 50 meters below the surface). This localization may be distinguished by the abundant pyrite mineralization with a small amount of arsenopyrite. It is composed of melanterite, small amounts of jarosite, and amorphous Fe oxyhydroxides, as well as bukovskýite, which stands for a characteristic component of this paragenesis. Bukovskýite is a relatively rarely secondary iron arsenate mineral. It is especially known from post-mining dumps (Novák *et al.* 1967; Loun *et al.* 2010; Haffert *et al.* 2010; Kocourková *et al.* 2011; Jelenová *et al.* 2018), as a product of hydrometallurgical processes (Ugarte and Monhemius 1992; Márquez *et al.* 2006). The mineral was also found in arsenic-rich tropical soils in the Ashanti region in Ghana (Bowell 1994) and as an accessory phase crystallizing from acid mine waters (Leblanc *et al.* 1996; Gieré *et al.* 2003; Triantafyllidis and Skarpelis 2006, Drahota and Filippi 2009). Crystallization of bukovskýite in Radzimowice is connected with oxidation of fine-grained pyrite intergrown with arsenopyrite. Oxidation of iron sulphide leads to the formation of Fe^{2+} ions (1). Then these ions undergo oxidation to Fe^{3+} ions (2).

(1) $FeS_2 + 3.5O_2 + H_2O = Fe^{2+} + 2SO_4^{2-} + 2H^+$
(2) $Fe^{2+} + 0.25O_2 + H^+ = Fe^{3+} + 0.5H_2O$

The Fe^{3+} ions are characterized by high oxidative potential and are the reason of fast decomposition of pyrite and arsenopyrite (3, 4):

(3) $FeS_2 + 14Fe^{3+} + 8H_2O \rightarrow 15Fe^{2+} + 2SO_4^{2-} + 16H^+$
(4) $FeAsS + 13Fe^{3+} + 8H_2O \rightarrow 14Fe^{2+} + SO_4^{2-} + 16H^+ + AsO_4^{3-}$,

This leads to the strong acidification of the environment and the release of significant amounts of sulphate, arsenate, and iron divalent ions (DeSisto *et al.* 2011). In these conditions, melanterite crystallizes,

as a mineral characteristic of environments with low pH (Frau 2000). Based on field observations in New Zealand (Mains and Craw 2005) and thermodynamic data (Gaskova *et al.* 2008) it can be assumed that after the crystallization of melanterite, the reaction of this mineral with arsenate ions in presence and formation of bukovskýite is coming up to (5):

(5) $2FeSO_4 \cdot 7H_2O + AsO_4^{3-} + 3H^+ + H_2O \rightarrow Fe_2(AsO_4)(SO_4)(OH) \cdot 7H_2O + SO_4^{2-} + 4H^+ + 7H_2O$

Coexistence of bukovskýite with melanterite points to the high activity of sulphate ions and low pH of the environment. A similar situation occurs, e.g., in Getchell mine, USA (Bowell and Parshley 2005), where bukovskýite coexists with pickeringite, halotrichite, melanterite, and jarosite. The thermodynamic calculations of Majzlan *et al.* (2012) conducted for bukovskýite from Kaňk near Kutná Hora and the observations of Kocourková-Víšková *et al.* (2015) confirm the observations from Radzimowice: the formation of bukovskýite is caused by high activity of sulphate and arsenate ions in a very narrow pH range (ca. 2.0–3.5). Majzlan (2020) indicates that bukovskýite is formed from the gels with high arsenic, sulphur and iron concentrations. No such relationship has been observed in Radzimowice. This may indicate that the formation of bukovskýite follows different patterns.

The second mineral assemblage of iron arsenates is characterized by the lack of easily water-soluble melanterite. Such paragenesis is located in the abandoned mine galleries of level III B (about 100 meters below the surface level) where the arsenopyrite mineralization (with the small amounts of pyrite) is exposed. The most characteristic components of this paragenesis are scorodite, pitticite, kaňkite and small amounts of zýkaite. These minerals are associated with hydroniumjarosite, schwertmannite, and amorphous iron oxyhydroxides.

Scorodite in this paragenesis usually forms earthy masses covering galleries and dripstones up to a few centimetres in length. Direct occurrence of scorodite on weathering pyrite-arsenopyrite intergrowths was not observed. It is probably due to very high amounts of groundwaters dribbling on the mine galleries' surfaces, which perpetually removes the products of oxidation of sulphide minerals. Only at a further distance from the decomposing sulphides scorodite may arise from a solution rich in Fe^{3+}, SO_4^{2-} and AsO_4^{3-} ions, according to the reaction (simplified) proposed by Debekaussen *et al.* (2001):

(6) $4AsO_4^{3-} + 12H^+ + 4Fe^{3+} + 3SO_4^{2-} + 8H_2O \rightarrow 4FeAsO_4 \cdot 2H_2O\downarrow + 12H^+ + 3SO_4^{2-}$.

This path of scorodite crystallization is responsible for the formation of monomineral dripstones and aggregates with a size of up to several cm. The coexistence of scorodite and pitticite may indicate that some of the scorodite is formed as a result of the transformation of the amorphous phase. The overgrowth of these phases in dripstones and small aggregates has been observed many times. The high sulfur content in the scorodite also indicates its relationship with pitticite. It should be noted that the process of scorodite crystallization can be much more complicated. The formation of this mineral can take place through the transformation of the precursor under the influence of arsenate ions present in the solution (e.g., Rong et al. 2020; Paktunc *et al.* 2008). This type of reaction has been reported by various authors (e.g., Rong et al. 2020; Paktunc *et al.* 2008). But the synthesis of scorodite has always been carried out at relatively high temperatures (70–90°C). The conditions in the abandoned mine in Radzimowice are totally different (e.g., constant temperature around 9°C). As a result, this method of scorodite formation seems unlikely. Such conditions are confirmed by the presence of kaňkite. This mineral is formed at moderate temperatures and high humidity (Majzlan *et al.* 2016). The coexistence of kaňkite with pitticite and the increased sulfur content may indicate that the kaňkite forming fine aggregates as a product of crystallization from amorphous pitticite. This model of kaňkite formation is consistent with observations from other mines (Jelenová *et al.* 2021). In the case of large aggregates, with a diameter of up to 40 cm, we suggest that the kaňkite precipitates in places where the solution, rich in arsenic ions, slowly seeps and evaporates.

Paktunc *et al.* (2008) and Paktunc and Bruggeman (2010) demonstrate, that higher solubility of scorodite takes place at low and high pH (i.e. <2 and >6), with the minimum solubility around pH 3–4. These results are comparable to those presented by Krause and Ettel (1989). The coexistence of scorodite accumulations with amorphous iron oxyhydroxides may indicate a periodic change of the crystallization conditions of the second mineral assemblage.

The increase of underground waters' pH (e.g., due to enlarged supply in humid seasons) may lead to the incongruent dissolution of this mineral (7):

(7) $FeAsO_4\,2H_2O + H_2O = H_2AsO_4^- + Fe(OH)_3\downarrow + H^+$.

The last reaction leads to the formation of amorphous iron oxyhydroxides, mainly ferrihydrite (e.g., Dove and Rimstidt 1985; Bluteau and Demopoulos 2007). This mineral is the main phase that arises in high amounts in the environment where the pH is over 5.5 (Kim *et al.* 2002; Murad and Rojík 2003; Kim and Kim 2004; Parviainen *et al.* 2012).

In comparison to crystalline scorodite, amorphous pitticite is characterized by lower stability. This phase dissolves already with the small decrease in the concentration of arsenate ions (Robins 1987; Chukhlantsev 1956; Langmiur *et al.* 2006).

Jarosite is a mineral characteristic of waters of low pH and high concentration of sulphate ions (Stahl *et al.* 1993; Baron and Palmer 1996; Nordstrom and Alpers 1999; Dutrizac and Jambor 2000; Norlund *et al.* 2010; Tang *et al.* 2020). The crystallization of scorodite according to reaction (6) leads to the increasing activity of sulphate ions in solution and a further drop of pH of the environment. This promotes the formation of favourable conditions for the crystallization of hydroniumjarosite which forms from the mine waters collected at the bottom of the gallery of level III B. The measured pH of these waters oscillates in the range of 1.95–2.19. Also, the presence of schwertmannite points to the low pH of the formation environment of the second paragenesis. This mineral is a characteristic element crystallizing from acid mine drainage of low pH (3–4) and rich in sulphate ions (1000–3000 mg/l) (Bigham *et al.* 1994, 1996; Bigham and Nordstrom 2000, Knorr and Blodau 2007; Yu *et al.* 2002; Aloune *et al.* 2015; Wang *et al.* 2020). The presence of this type of water was confirmed in the sites of crystallization of the second assemblage of iron arsenates (Cłapa *et al.* 2019). According to Majzlan *et al.* (2015) the presence of zýkaite in this mineral assemblage also confirmed a low pH and very high activities of arsenate and sulphate ions.

Minerals of the erythrite-annabergite-hörnesite series are the rarest secondary arsenic minerals which crystallize in the abandoned mine in Radzimowice. Supergene Co-Ni-Mg arsenates of the erythrite-annabergite-hörnesite solid solution occur in another mine gallery of the IIIB exploitation level, about 500 m from second paragenesis Their crystallisation is related to the decomposition of Co-Ni arsenides and cobalt rich arsenopyrite. Weathering of these minerals does not cause a significant reduction in pH. This is because the decomposition of Co-Ni arsenides does not release large amounts of sulphuric acid but only poorly dissociated arsenic acid. Moreover, the presence of dolomite has a buffering effect on the pH. Mg^{2+} ions are supplied to the system from weathering ore-vein dolomite. The formation of the erythrite-annabergite-hörnesite solid solution is very similar to the mechanism described by Markl *et al.* (2014). According to data obtained by Langmuir *et al.* (1999) and Mahoney *et al.* (2007) these arsenates crystallized from slightly acidic media (pH ~5–6). These data were confirmed by Yuan *et al.* (2005), who proved that the solubility of annabergite decreases with increasing pH (minimal at pH = 9). The same relationship was confirmed for erythrite (Zhu *et al.* 2013). Crystallisation of hörnesite under neutral or alkalescent pH conditions is also confirmed by the existence of hörnesite in soils with high arsenic content (Voigt *et al.* 1996; Foster *et al.* 1997).

CONCLUSIONS

The mines taken into consideration in the research differ in terms of their environmental conditions, which entails heterogeneity in the composition of mineral paragenesis. Three main assemblages containing iron arsenates were determined. The first one, located at the II exploitation level, is composed of bukovskýite, melanterite, jarosite, and Fe oxyhydroxides. Such a mineral assemblage indicates low pH inside the second mine level. Weathering conditions were favourable for the high activity of sulphate and arsenate ions which lead to the crystallization of bukovskýite. The second assemblage of secondary arsenic minerals is located at the IIIB level of the abandoned mine. This assemblage consists of scorodite, kaňkite, pitticite, zýkaite associated with hydroniumjarosite, schwertmannite and amorphous iron oxyhydroxides. The geochemical conditions are different from these characterizing the II mine level, which is evidenced by the lack of the easily water-soluble minerals like melanterite. There is a similarity in the pH of both assemblages, which is low, and on the third level, it oscillates around 2. The existence of amorphous iron oxyhydroxides (ferrihydrite), which are stable at pH>5.5, along with scorodite being most stable around 3–4 pH, suggest that environmental conditions were changing periodically. These changes promote phase transformations in this mineral assemblage. The Co-Ni arsenates crystallize in small zones where completely different conditions prevail. Arsenates of the erythrite-annabergite-hörnesite solid solution are produced by the decomposition of primary Co-Ni arsenides and Co rich arsenopyrite. This process does not cause a significant pH reduction. For this reason, these minerals crystallize under slightly acidic to neutral or alkalescent pH conditions.

Acknowledgements

The authors would like to thank Dr. Petr Drahota from the Charles University, Institute of Geochemistry, Mineralogy

and Mineral Resources and Dr. hab. Bożena Gołębiowska from AGH University of Science and Technology, Department of Mineralogy, Petrology and Geochemistry for their valuable reviews and corrections that provide essential improvements to the article. Research was financed with the funds of the Department of Geochemistry, Mineralogy and Petrology, University of Warsaw.

REFERENCES

Aloune, S.H. and Hiroyoshi, N., Ito M. 2015. Stability of As(V)-sorbed schwertmannite under porphyry copper mine conditions. *Minerals Engineering*, **74**, 51–59.

Baranowski, Z. 1988. Lithofacies characteristics of trench-fill metasediments in the Radzimowice Slate (Paleozoic, Sudetes, SW Poland). *Annales Societatis Geologorum Poloniae,* **58**, 325–383.

Baron, D. and Palmer, C.D. 1996. Solubility of jarosite at 4–35ºC. *Geochimica et Cosmochimica Acta*, **60**, 185–195.

Bigham, J.M., Carlson, L. and Murad, E. 1994. Schwertmannite, a new iron oxyhydroxysulfate from Pyhäsalmi, Finland and other localities. *Mineralogical Magazine*, **58**, 641–648.

Bigham, J.M., Schwertmann, U., Traina, S.J., Winland, R.L. and Wolf, M. 1996. Schwertmannite and the chemical modeling of iron in acid sulfate waters. *Geochimica et Cosmochimca Acta*, **60**, 2111–2121.

Bigham, J.M. and Nordstrom, D.K. 2000. Iron and aluminium hydroxysulfates from acid sulfate waters, in: Sulfate Minerals: Crystallography, Geochemistry and Environmental Significance. *Reviews in Mineralogy and Geochemistry*, **40**, 351–403.

Bluteau, M.-C. and Demopoulos, G.P. 2007. The incongruent dissolution of scorodite – Solubility kinetics and mechanism. *Hydrometallurgy*, **87**, 163–177.

Bowell, R.J. 1994. Sulphide oxidation and arsenic speciation in tropical soils. *Environmental Geochemistry and Health*, **16**, 84.

Bowell, R.J. and Parshley, J.V. 2005. Control of pit-lake water chemistry by secondary minerals, Summer Camp pit, Getchell mine, Nevada. *Chemical Geology*, **215**, 373–385.

Čech, J., Jansa, J. and Novák, F. 1976. Kaňkite, $FeAsO_4 \cdot 3.5H_2O$, a new mineral. *Neues Jahrbuch für Mineralogie Monatshefte*, **5**, 426–436.

Čech, J., Jansa, J. and Novák, F. 1978. Zýkaite, $Fe^{3+}_4(AsO_4)_3(SO_4)(OH) \cdot 15H_2O$, a new mineral. *Neues Jahrbuch für Mineralogie Monatshefte*, **3**, 134–144.

Chukhlantsev, V.G. 1956. The solubility products of a number of arsenates. *Journal of Analytical Chemistry of the USSR*, **11**, 565–571.

Cłapa, T., Narożna, D., Siuda, R., Borkowski, A., Selwet, M. and Mądrzak, C. 2019. Diversity of Bacterial Communities in the Acid Mine Drainage Ecosystem of an Abandoned Polymetallic Mine in Poland. *Polish Journal of Environmental Studies*, **28**, 2109–2119.

Debekaussen, R., Droppert, D. and Demopoulos, G.P. 2001. Ambient pressure hydrometallurgical conversion of arsenic trioxide to crystalline scorodite. *Canadian Institute of Mining and Metallurgy Bulletin*, **94**, 116–122.

DeSisto, S.L., Jamieson, H.E. and Parsons, M.B. 2011. Influence of hardpan layers on arsenic mobility in historical gold mine tailings. *Applied Geochemistry,* **26**, 2004–2018.

Dove, P.M and Rimstidt, J.D. 1985. The solubility and stability of scorodite, $FeAsO_4 \cdot 2H_2O$. *American Mineralogist*, **70**, 838–844.

Drahota, P and Filippi, M. 2009. Secondary arsenic minerals in the environment: A review. *Environmental International*, **35**, 1243–1255.

Dunn, P.J. 1982. New data for pitticite and a second occurrence of yukonite at Sterling Hill, New Jersey. *Mineralogical Magazine*, **46**, 261–264.

Dutrizac, J.E. and Jambor, J.L. 2000. Jarosite and their application in hydrometallurgy. In: Alpers, C.N. and Jambor, J.L. (Eds), Sulfate Minerals: Crystallography. Geochemistry and Environmental Significance, Vol. 40. *Mineralogical Society of America*, **443**, 405–452.

Dziekoński, T. 1972. Wydobywanie i metalurgia kruszców na Dolnym Śląsku od XIII do połowy XX wieku. *PAN-IHKM, Zakład Narodowy im. Ossolińskich, Wrocław-Warszawa-Gdańsk*, **420**, 1–420.

Fiedler, H. 1863. Die Mineralien Schlesiens mit Berücksichtigung der angrenzenden Länder, 121 pp. Breslau. [In German].

Filippi, M., Goliáš, V. and Pertold, Z. 2004. Arsenic in contaminated soils and anthropogenic deposits at the Mokrsko, Roudný, and Kašperské Hory gold deposits, Bohemian Massif (CZ). *Environmental Geology*, **45**, 716–730.

Foster, A.L., Brown Jr., G.E., Tingle, T.N., Parks, G.A., Voigt, D.E. and Brantley, S.L. 1997. XAFS determination of As speciation in weathered mine tailings and contaminated soil from California, USA. *Journal de Physique IV (Proceedings*), **7**, 815–816.

Frau, F. 2000. The formation-dissolution-precipitation-cycle of melanterite at the abandoned pyrite mine of Genna Luas in Sardinia, Italy: environmental implications. *Mineralogical Magazine*, **64**, 995–1006.

Frost, R.L., Scholz, R., Jirásek, J. and Belotti, F.M. 2015. An SEM-EDX and Raman spectroscopic study of the fibrous arsenate mineral liskeardite and in comparison with other arsenates kaňkite, scorodite and yvonite. *Spectrochimica Acta Part A: Molecural and Biomelecular Spectroscopy*, **151**, 566–575.

Frost, R.L., Xi Y., Palmer, S.J. and Tan, K. 2011. Molecular structural studies of the amorphous mineral pitticite Fe, AsO_4, SO_4, H_2O. *Journal of Molecular Structure*, **1005**, 78–82.

Frost, R.L., Xi, Y., Tan, K., Millar, G.J. and Palmer, S.J. 2012. Vibrational spectroscopic study of the mineral pitticite Fe, AsO_4, SO_4, H_2O. *Spectrochimica Acta Part A: Molecular and Biomolecular Spectroscopy*, **85**, 173–178.

Gaskova, O.L., Shironosova, G.P. and Bortnikova, S.B. 2008. Thermodynamic Estimation of the Stability Field of Bukovskýite, an Iron Sulfoarsenate. *Geochemistry International*, **1 (46)**, 85–91.

Gieré, R., Sidenko, N.V. and Lazareva, E.V. 2003. The role of secondary minerals in controlling the migration of arsenic and metals from high-sulfide wastes (Berikul gold mine, Siberia). *Applied Geochemistry*, **18**, 1347–1359.

Gomez, A.M., Assaaoudi, H., Becze, L., Cutler, J.N. and Demopoulos, G.P. 2010. Vibrational spectroscopy study of hydrothermally produced scorodite ($FeAsO_4 \cdot 2H_2O$), ferric arsenate sub-hydrate (FAsH; $FeAsO_4 \cdot 0.75H_2O$) and basic ferric arsenate sulfate (BFAS; $Fe[(AsO_4)_{1-x}(SO_4)x(OH)_x] \cdot wH_2O$). *Journal of Raman Spectroscopy*, **41**, 212–221.

Haffert, L., Craw, D. and Pope, J. 2010. Climatic and compositional controls on secondary arsenic mineral formation in high-arsenic mine wastes, South Island, New Zealand. *New Zealand Journal of Geology and Geophysics*, **53**, 91–101.

Haydukiewicz, A. and Urbanek, Z. 1986. Zmetamorfizowane skały dewońskie we wschodniej części jednostki Bolkowa (Góry Kaczawskie). *Geologia Sudetica*, **20**, 185–196. [In Polish]

Hering, J. and Kneebone, P.E. 2002. Biogeochemical controls on arsenic occurrence and mobility in water supplies. In: Frankenberger, W. (Ed.), *Environmental Chemistry of Arsenic. Marcel Dekker, New York*, **159**, 155–181.

Holeczek, J. and Janeczek, J. 1991. Pseudomalachite from Radzimowice and some comments on its occurrence in Miedzianka (Sudetes Mts.). *Mineralogia Polonica*, **22 (1)**, 17–26.

Jelenová, H., Majzlan, J., Amoako, F.Y. and Drahota, P. 2018. Geochemical and mineralogical characterization of the arsenic-, iron-, and sulfur-rich mining waste dumps near Kaňk, Czech Republic. *Applied Geochemistry,* **97**, 247–255.

Jelenová, H., Drahota, P., Falteisek L. and Culka, A. 2021. Arsenic-rich stalactites from abandoned mines: Mineralogy and biogeochemistry. Applied Geochemistry, **129**, 104960.

Johnson, D.B., Dybowska, A., Schofield, P.F., Herrington, R.J., Smith, S.L. and Santos, A.L. 2020. Bioleaching of arsenic-rich cobalt mineral resources, and evidence for concurrent biomineralisation of scorodite during oxidative bio-processing of skutterudite. *Hydrometallurgy*, **195**, doi. org/10.1016/j.hydromet.2020.105395.

Kato, A., Matsubara, S., Nagashima, K., Nakai, I. and Shimizu, M. 1984. Kaňkite from the Suzukura mine, Kenzan city, Yamanashi Prefecture, Japan. *Mineralogical Journal*, **12(1),** 6–14.

Kim, J.J., Kim, S.J. and Tazaki, K. 2002. Mineralogical characterization of microbial ferrihydrite and schwertmannite, and non-biogenic Al-sulphate precipitates from acid mine drainage in the Donghae mine area, Korea. *Environmental Geology*, **42**, 19–31.

Kim, J.J. and Kim, S.J. 2004. Seasonal factors controlling mineral precipitation in the acid mine drainage at Donghea coal mine, Korea. *Science of the Total Environment*, **325**, 181–191.

Knorr, K.-H. and Blodau, C. 2007. Controls on schwertmannite transformation rates and products. *Applied Geochemistry***, 22**, 2006–2015.

Kocourková, E., Cempírek J. and Losos Z. 2008. Kaňkit z Dlouhé Vsi u Havlíčkova Brodu. *Acta rerum naturalium*, **4**, 7–12.

Kocourková, E., Sracek, O., Houzar, S., Cempírek, J., Losos, Z., Filip, J. and Hršelová, P. 2011. Geochemical and mineralogical control on the mobility of arsenic in a waste rock pile at Dlouhá Ves, Czech Republic. *Journal of Geochemical Exploration*, **110**, 61–73.

Kocourková-Víšková, E., Loun, J., Sracek, O., Houzar S. and Filip J. 2015. Secondary arsenic minerals and arsenic mobility in a historical waste rock pile at Kaňk near Kutná Hora, Czech Republic. *Mineralogy and Petrology*, **109**, 17–33.

Kozdrój, W., Krentz, O. and Opletal, M. 2001. Comments on the Geological Map Lausitz-Izera-Karkonosze, 1:100 000. *Polish Geological Institute*, Warszawa.

Krause, E. and Ettel, V.A. 1989. Solubilities and stabilities of ferric arsenate compounds. *Hydrometallurgy*, **22**, 311–337.

Kubisz, J. 1971. Studies on synthetic alkali-hydronium jarosites II: thermal investigations. *Mineralogia Polonica*, **2**, 51–60.

Langmuir, D., Mahoney, J., MacDonald, A and Rowson, J. 1999. Predicting arsenic concentrations in the porewaters of buried uranium mill tailing. *Geochimica et Cosmochimica Acta*, **63**, 3379–3394.

Langmuir, D., Mahoney, J. and Rowson, J. 2006. Solubility products of amorphous ferric arsenate and crystalline scorodite ($FeAsO_4 \cdot 2H_2O$) and their application to arsenic behavior in buried mine tailings. *Geochimica et Cosmochimica Acta*, **70**, 2942–2956.

Leblanc, M., Achard, B., Ben Othman, D. and Luck, J.M. 1996. Accumulation of arsenic from acidic mine waters by ferruginous bacterial accretions (stromatolites). *Applied Geochemistry*, **11**, 541–554.

Li, H., Wang, N., Xiao, T., Zhang, X., Wang, J., Tang, J. and Quan, H. 2021. Sorption of arsenate(V) to naturally occurring secondary iron minerals formed at different conditions: The relationship between sorption behavior and surface structure. *Chemosphere*, **285**, 131–525.

Loun, J. Pauliš, P. Novák, F., Plášil, J. and Ševců, J. 2010. Supergene As mineralization of the mine dump Stará Plime at Kaňk near Kutná Hora (Czech Republic). *Bulletin mineralogicko-petrologického oddělení Národního muzea v Praze*, **18**, 73–77. [In Czech with English abstract]

Loun, J., Čejka, J., Sejkora, J., Plášil, J., Novák, M., Frost, R.L., Palmer, S. and Keeffe, E. 2011. A Raman spectroscopic study of bukovskýite $Fe_2(AsO_4)(SO_4)(OH) \cdot 7H_2O$, a

mineral phase with a significant role in arsenic migration. *Journal of Raman Spectroscopy*, **42**, 1596–1600.

Machowiak, K., Amstrong, R., Kryza, R. and Muszyński, A. 2008. Late-orogenic magmatism in the Central European Variscides: SHRIMP U-Pb zircon age constraints from the Żeleźniak intrusion, Kaczawa Mountains, West Sudetes. *Geologia Sudetica*, **40**, 1–18.

Mahoney, J., Slaughter, M., Langmuir, D. and Rowson, J. 2007. Control of As and Ni release from a uranium mill tailings neutralization circuit: Solution chemistry, mineralogy and geochemical modeling of laboratory study results. *Applied Geochemistry*, **22**, 2758–2776.

Mains, D and Craw, D. 2005. Composition and mineralogy of historic gold processing residues, east Otago. New Zeland. *New Zeland Journal of Geology and Geophysics*, **48**, 641–647.

Majzlan, J., Łazić B., Armbruster, T., Johnson, M.B., White, M.A., Fisher, R.A., Plášil, J., Loun, J., Škoda, R. and Novák, M. 2012. Crystal structure, thermodynamic properties, and paragenesis of bukovskýite, $Fe_2(AsO_4)(SO_4)(OH)\cdot 9H_2O$. *Journal of Mineralogical and Petrological Sciences*, **107 (3)**, 133–148.

Majzlan, J., Amoako, F.Y., Kindlová, H. and Drahota, P. 2015. Thermodynamic properties of zýkaite, a ferric sulfoarsenate. *Applied Geochemistry*, **61**, 294–301.

Majzlan, J., Palatinus L. and Plášil, J. 2016. Crystal structure of $Fe_2(AsO_4)(HAsO_4)(OH)(H_2O)_3$, a dehydratation product of kaňkite. European Journal of Mineralogy, **28**, 63–70.

Majzlan, J. 2020. Processes of metastable-mineral formation in oxidation zones and mine waste. Mineralogical Magazine, **84**, 367–375.

Manecki, A. 1962. Mineralizacja miedzią występująca w rejonie Bukowej Góry koło Radzimowic (Dolny Śląsk). *Sprawozdania z Posiedzeń Komisji Nauk Mineralogicznych PAN Oddział w Krakowie*, **2**, 460–461.

Manecki, M. 1965. Mineralogical and petrographical study of ore veins of the vicinity of Wojcieszów (Lower Silesia). *Prace Mineralogiczne*, **2**, 1–90. [In Polish with English summary]

Markl, G., Marks, M.A.W., Derrey, I. and Gühring, J.-E. 2014. Weathering of cobalt arsenides: Natural assemblages and calculated stability reactions among secondary Ca-Mg-Co arsenates and carbonates. *American Mineralogist*, **99**, 44–56.

Márquez, M., Gaspar, J., Bessler, K.E. and Mageda, G. 2006. Process mineralogy of bacterial oxidized gold ore in São Bento Mine (Brasil). *Hydrometallurgy*, **83**, 114–123.

Matschullat, J. 2000. Arsenic in the geosphere – a review. *Science of the Total Environment*, **249**, 297–312.

Mikulski, S.Z. 2003. Proceedings of the 7th Biennial SGA meeting, Athens, Greece, 24–28 August. Multiple episodes of magmatic and hydrothermal activity at the Radzimowice gold deposit in the Sudetes Mountains (Bohemian Massif, Poland), 339–342. Mineral exploration and sustainable development; Millpress.

Mikulski, S.Z. 2005. Geological, mineralogical and geochemical characteristics of the Radzimowice Au-As-Cu deposit from the Kaczawa Mountains (Western Sudetes, Poland): an example of the transition of porphyry and epithermal style. *Mineralium Deposita*, **39**, 904–920.

Mikulski S.Z. 2007. The late Variscan gold mineralization in the Kaczawa Mountains, Western Sudetes. *Polish Geological Institute Special Papers*, **22**, 1–162.

Mikulski, S.Z. 2011. Gold deposits in Kaczawa Mountains, West Sudetes, SW Poland. *Archivum Mineralogiae Monograph*, **2**, 63–83.

Mikulski, S.Z and Muszyński, A. 2012. Petzite (Ag_3AuTe_2) – a new telluride mineral from the Radzimowice deposit (Sudetes, SW Poland). *Mineralogical Society of Poland – Special Papers*, **40**, 103–104.

Mikulski, S.Z. and Williams I.S. 2014. Zircon U-Pb dating of igneous rocks in the Radzimowice and Wielisław Złotoryjski auriferous polymetallic deposits, Sudetes, SW Poland. *Annales societatis Geologorum Poloniae*, **48**, 213–233.

Morin, G. and Calas, G. 2006. Arsenic in soils, mine tailings, and former industrial sites. *Elements*, **2**, 97–101.

Murad, E. and Rojík, P. 2003. Iron-rich precipitates in a mine drainage environment: Influence of pH on mineralogy. *American Mineralogist*, **88**, 1915–1918.

Nordstrom, D.K. and Alpers, C.N. 1999. Geochemistry of acid mine waters. In: Plumlee, G.S., Logsdon, M.J. (Eds.). *The Environmental Geochemistry of Mineral Deposits, Part A: Processes, Techniques and Health Issues, Reviews in Economic Geology, Vol. 6A. Society of Economic Geologists*, **136**, 133–160.

Norlund, K.L.I., Baron, C. and Warren, L.A. 2010. Jarosite formation by an AMD sulphide-oxidizing environmental enrichment: implications for biomarkers on Mars. *Chemical Geology*, **275**, 235–242.

Novák, F., Povondra, P. and Vtělenský, J. 1967. Bukovskýite, $Fe^{2+}_2(AsO_4)(SO_4)(OH)\cdot 7H_2O$, from Kaňk, near Kutná Hora – a new mineral. *Acta Universitatis Carolinae – Geologica*, **4**, 297–325.

Ondruš, P., Skála, R., Viti, C., Veselovský, F., Novák, F. and Jansa, J. 1999. Parascorodite, $FeASO_4\cdot 2H_2O$ – a new mineral from Kaňk near Kutná Hora, Czech Republic. *American Mineralogist*, **84**, 1439–1444.

Paktunc, D., Dutrizac, J. and Gertsman, V. 2008. Synthesis and phase transformations involving scorodite, ferric arsenate and arsenical ferrihydrite: implications for arsenic mobility. *Geochimica et Cosmochimica Acta*, **72**, 2649–2672.

Paktunc, D. and Bruggeman, K. 2010. Solubility of nanocrystalline scorodite and amorphous ferric arsenate: implications for stabilization of arsenic in mine wastes. *Applied Geochemistry*, **25**, 674–683.

Parafiniuk, J. and Siuda R. 2006. Schwertmannite precipitated from acid mine drainage in the Western Sudetes (SW Po-

land) and its arsenate sorption capacity. *Geological Quarterly*, **50**, 475–486.

Parafiniuk, J., Siuda, R. and Borkowski, A. 2016. Sulphate and arsenate minerals as environmental indicators in the weathering zones of selected ore deposits, Western Sudetes, Poland. *Acta Geologica Polonica*, **66** (3), 493–508.

Parviainen, A., Lindsay, M.B.J., Pérez-López, R., Gibson, B.D., Ptacek, C.J, David W. Blowes, D.W. and Loukola-Ruskeeniemi, K. 2012. Arsenic attenuation in tailings at a former Cu-W-As mine, SW Finland. *Applied Geochemistry*, **27**, 2289–2299.

Paulo, A. and Salomon, W. 1974. Contribution to the knowledge of a polymetallic deposit at Stara Góra. *Kwartalnik Geologiczny*, **18** (2), 266–276. [In Polish with English summary]

Qi, X., Li, Y., Wei, L., Hao, F., Zhu, X., Wei, Y., Li, K. and Wang, H. 2020. Disposal of high-arsenic waste acid by the stepwise formation of gypsum and scorodite. *Royal Society of Chemistry Advances*, **10**, 29–42.

Robins, R.G. 1987. Solubility and stability of scorodite, $FeAsO_4{\cdot}2H_2O$: Discussion. *American Mineralogist*, **72**, 842–844.

Rong,, Z., Tang, X., Wu, L., Chen, X., Dang, W. and Wang, Y. 2020. A novel method to synthesize scorodite using ferrihydrite and its role in removal and immobilization of arsenic. *Journal of Materials Research and Technology.* **198**, 106936.

Salzsauler, K.A., Sidenko, N.V. and Sherriff, B.L. 2005. Arsenic mobility in alternation products of sulfide-rich, arsenopyrite-bearing mine wastes, Snow Lake, Manitoba, Canada. *Applied Geochemistry*, **20**, 2303–2314.

Siuda, R. 2004. Iron arsenates from Stara Góra deposit at Radzimowice in Kaczawa Mountains, Poland – a preliminary report. *Mineralogical Society of Poland – Special Papers*, **24,** 345–348.

Siuda, R. and Kruszewski, Ł. 2005. Arsenate mottramitte from the Stara Góra deposit (Kaczawa Mts., Poland) – preliminary report. *Mineralogical Society of Poland – Special Papers*, **26**, 262–265.

Siuda, R and Kruszewski, Ł. 2013. Recently formed secondary copper minerals as indicators of geochemical conditions in an abandoned mine in Radzimowice (SW Poland). *Geological Quarterly*, **57**, 583–600.

Smedley, P.L. and Kinniburgh, D.G. 2002. A review of the source, behaviour and distribution of arsenic from mine tailings. *Applied Geochemistry*, **17**, 517–568.

Stahl, R.S., Fanning, D.S. and James, B.R. 1993. Goethite and Jarosie precipitation from ferrous sulfate solutions. *Soil Science Society of America Journal*, **57**, 280–282.

Stauffacher, J. 1916. Der Goldgangdistrikt von Altenberg in Schlesien. *Zeitschrift für praktische Geologie*, **23**, 53–88.

Sylwestrzak, H. and Wołkowicz, K. 1985. A new assemblage of Sn-W-Mo minerals from Stara Góra (Lower Silesia) and its genetic significance. *Przegląd Geologiczny*, **33**, 73–75. [In Polish with English summary]

Tang, Y., Xie, Y., Lu, G., Ye, H., Dang, Z., Wen, Z. and Yi, X. 2020. Arsenic behavior during gallic acid-induced redox transformation of jarosite under acidic conditions. *Chemosphere*, **255**, 12693.

Traube, H. 1888. Die Minerale Schlesiens. 286 pp. J.U. Kern's Verlag (Max Miller); Breslau. [In German]

Triantafyllidis, S. and Skarpelis, N. 2006. Mineral formation in an acid pit lake from a high-sulfidation ore deposit: Kirki, NE Greece. *Journal of Geochemical Exploration*, **88**, 68–71.

Ugarte, F.J.G. and Monhemius, A.J. 1992. Characterisation of high-temperature arsenic-controlling residues from hydrometallurgical processes. *Hydrometallurgy*, **30 (1–3)**, 69–86.

Urbanek, Z., Baranowski Z. 1986. Revision of age of the Radzimowice schists from the Góry Kaczawskie Western Sudetes. *Annales Societatis Geologorum Poloniae*, **56**, 399–408.

Voigt, D.E., Brantley, S.L. and Hennet, R.J.-C.1996. Chemical fixation of arsenic in contaminated soils. *Applied Geochemistry*, **11**, 633–643.

Wang, Y., Gao, M., Huang, W., Wang, T. and Liu, Y. 2020. Effects of extreme pH conditions on the stability of As(V)-bearing schwertmannite. *Chemosphere*, **251**, 126427.

Welch, A.H., Westjohn, D.B., Helsel, D.R. and Wanty, R.B. 2000. Arsenic in ground water of the United States: occurrence and geochemistry. *Groundwater*, **38**, 589–604.

Yu, J.Y., Park, M. and Kim, J. 2002. Solubilities of synthetic schwertmannite and ferrihydrite. *Geochemical Journal*, **36**, 119–132.

Yuan, T.C., Jia, Y.F. and Demopoulos, G.P. 2005. Synthesis and solubility of crystalline annabergite $Ni_3(AsO_4)_2{\cdot}8H_2O$. *Canadian Metallurgical Quarterly*, **44**, 449–456.

Zhu, Y.N., Zhang, X.H., Chen, Y.D., Zeng, H.H., Liu, J., Liu, H.L. and Wang, X.M. 2013. Characterization, dissolution and solubility of synthetic erythrite $[Co_3(AsO_4)_2{\cdot}8H_2O]$ and annabergite $[Ni\ (AsO_4)_2{\cdot}8H_2O]$ at 25 °C. *Canadian Metallurgical Quarterly*, **51**, 7–17.

Zimnoch, E. 1965. New data about ore mineralization in Stara Góra deposit. *Biuletyn Geologiczny Wydziału Geologii UW*, **5**, 3–38 [In Polish].

Manuscript submitted: 23rd May 2022
Revised version accepted: 7th September 2022